Purification of antibody fragments by phenylboronate chromatography using a microfluidic device

Miguel Duarte Monteiro Ambrósio

Thesis to obtain the Master of Scientific Degree in:

Biotechnology

Supervisors: Prof. Ana Margarida Nunes da Mata Pires de Azevedo

MSc. André Nunes dos Santos Nascimento

Examination Committee:

Chairperson: Prof. Marília Clemente Velez Mateus

Supervisor: Prof. Ana Margarida Nunes da Mata Pires de Azevedo

Members of the committee: Prof. Ana Cristina Dias Cabral

November 2019

Preface

The work presented in this thesis was performed at the Institute for Bioengineering and Biosciences of Instituto superior Técnico (Lisbon, Portugal), during the period September-August 2019, under the supervision of Professor Ana Margarida Nunes da Mata Pires de Azevedo and André Nunes dos Santos Nascimento, within the frame of the FCT funded project PureMab.

Declaration

I declare that this document is an original work of my own authorship and that it fulfils all the requirements of the Code of Conduct and Good Practices of the Universidade de Lisboa.

Agradecimentos

Em primeiro lugar, gostaria de agradecer à minha orientadora Professora Ana Azevedo, por me ter aceite no seu grupo de investigação e por todos os conselhos dados no decorrer do desenvolvimento da tese, bem como as suas palavras de encorajamento. Os seus conhecimentos sobre fenilboronato foram decisivos para entender algo tão complexo. Gostaria também de agradecer ao meu co-orientador André Nascimento por me ter aceite em contexto do desenvolvimento da sua tese de doutoramento, pela sua disponibilidade e encorajamento nos momentos de desespero, típicos da investigação científica.

Em segundo lugar, queria agradecer a toda a gente do laboratório por me ter recebido da melhor forma. Obrigado à Sara Rosa pelos conselhos sobre fenilboronato, à Sara Rosa II e à Rita por toda ajuda no AKTA, ao Diogo pelos debates políticos e ao João e ao Jorge por questões gerais do laboratório. Um especial obrigado à Diva Mariana, com quem acabei por me tornar tão amigo. Os seus conselhos sobre o mestrado (e sobre a vida), neste último ano, foram fundamentais.

Agradeço ainda às companhias de almoço e after-work no Arco do cego, à companheira de escrita, com quem partilhei diversos momentos de desespero, Ana Catarina, e ao companheiro de mestrado e de conversas pseudo-intelectuais Arthur, o estrangeiro que me introduziu a Albert Camus. Obrigado a todos os meus amigos, especialmente às queridas amigas Cátia, Érica, Carolina, Mafalda e Tânia. Obrigado à Marta Mota por toda a amizade, apesar de constantemente me dizer que não sou o seu preferido.

Por último mas mais importante, queria agradecer à minha família por tudo: ao meu pai por manter a calma mesmo perante o apocalipse, à minha mãe por não manter a calma em circunstância nenhuma e por pensar que vou morrer à mínima queixa. Obrigado ao meu irmão pelos seus atrasos habituais de 3 horas, à Bia pelas caras de nojo e à minha tia pelas suas mensagens, mesmo quando não estou tão presente. Obrigado aos meus avós que, apesar de já não estarem presentes, guardo-os com tanto carinho. A todos eles, obrigado por fazerem de mim a pessoa que sou hoje, pelos momentos de amor e palavras de encorajamento. Finalmente, obrigado ao Gonçalo, por todo o apoio e carinho dado ao longo destes últimos anos. Os passeios habituais no paredão, ao final de um longo dia de trabalho, ajudaram muito na realização desta tese. Obrigado, ainda, por fazer questão de meter Taylor Swift a dar cada vez que entro no carro (devias parar). Are you calling me Ballet?

Abstract

Antibodies are glycoproteins used in a wide range of fields because of their affinity and specificity towards specific antigens. Alternatives to full-sized antibodies have also been developed, as antigen-binding fragments, which are today the most widely used. Despite their increasing popularity, there is no preferable method to purify these antibody derivates, since there is no universal affinity ligand. In the last years, phenylboronate has been successfully employed to capture monoclonal antibodies, due to its affinity to cis-diol groups, and, more recently, for binding to kappa Fab fragments.

In this work, the digestion protocol of human antibodies was initially optimized, with an increase of 41% in the antibody digestion yield obtained. Then, the possibility of using aminophenylboronate for purification of kappa and lambda classes of Fabs was thoroughly investigated. A microfluidic platform was used to screen different binding and elution conditions in a high throughput manner, followed by validation at macroscale. Several impurities related with the manufacturing process of Fabs were also studied. Overall, below ligand pKa, affinity binding, enhanced by charge transfer interactions, was the driving force for the adsorption process. Optimal binding of Fabs occurred at pH 5 and 7 for intermediate and lower concentrations of salt, respectively. At pH 9.2, electrostatic repulsion supressed affinity interactions. Due to the presence of different isotypes and subclasses and also due to polyclonal nature of the feed, Fabs were found in both flow-through and elution fractions. Further studies would be required to assess the behaviour of this ligand towards a monoclonal Fab.

Key words: aminophenylboronate, antigen-binding fragments, chromatography, microfluidics

Resumo

Os anticorpos são glicoproteínas que possuem um elevado grau de afinidade e especificidade para os antigénios, e por isso, são aplicados em diversas áreas. No entanto quando utilizados como terapêuticos, apresentam algumas limitações, pelo que têm sido desenvolvidas alternativas para anticorpos completos, com destaque para os fragmentos de ligação do antigénio (Fabs). No entanto, a ausência de um universal ligando de afinidade requer o desenvolvimento de novos métodos para a sua purificação.

Neste trabalho, o protocolo de digestão de anticorpos humanos foi inicialmente otimizado, levando ao aumento de 41% no rendimento do processo. Depois disso, a possibilidade de usar o ligando aminofenilboronato para a purificação das classes kappa e lambda de Fabs foi estudada, utilizando um dispositivo de microfluídica para o rastreio de diferentes condições cromatográficas, seguido da validação destes resultados à macro-escala. Realizou-se, ainda, o estudo da afinidade de várias impurezas, envolvidas na produção de fragmentos, para o ligando. Genericamente, abaixo do pKa do ligando, as ligações de afinidade, potenciadas por interações de transferência de carga, foram o fator dominante no processo de adsorção. Acima desse valor, repulsão electroestática suprimiu as interações de afinidade. Ligação maximizada dos Fabs para o fenilboronato foi verificada sob concentrações de sal intermédias e mais baixas a pH 5 e 7, respetivamente. Provavelmente associado a diferentes isotipos, os Fabs dividiram-se entre as frações que não ligaram à coluna e eluição, pelo que terão de ser realizar mais estudos para confirmar a possibilidade de utilização deste ligando para a sua purificação.

Palavras-chave: aminofenilboronato, fragmento de ligação do antigénio, cromatografia, microfluídica

Table of contents

List of tables

List of figures

List of abbreviations

Ab Antibody

AEX Anion exchange chromatography

APBA phenyl boronic acid

CDR Complementarity-determining region

CEX Cation exchange chromatography

CHO Chinese hamster ovary

CV Column volumes

DOE Design of experiments

DOL Degree of labelling

E Elution

Fab Antigen-binding fragment

Fc Fragment crystallizable region

FT Flow-through

HIC Hydrophobic interaction chromatography

IEX Ion exchange chromatography

Ig Immunoglobulin

IMAC Metal-ion affinity chromatography

mAb Monoclonal antibody

MMC Mixed-mode chromatography

pAb Polyclonal antibody

PBC phenylboronate chromatography

PBS Phosphate buffered saline

PDMS polydimethylsiloxane

pI Isoelectric point

SEC Size exclusion chromatography

Tris Tris (hydroxymethyl)aminomethane

1. Context and motivation

Antibodies are glycoproteins, naturally found in the human body, that can recognize and bind to a given antigen with a high degree of affinity and specificity. Because of these properties, immunoglobulins have been used for a wide range of applications, namely in biotechnology, pharmaceutical and medical fields[1]. However, their utilization has some limitations, including restricted penetration and homogenous distribution in target tissues and triggering of secondary immune reactions. They also present a prolonged half-life time, which can be a limiting factor for some applications. All these constrains are caused by the large molecular height of full-sized antibodies[2].

In the past decades, development of alternatives to monoclonal antibodies has gained relevance, particularly smaller proteins with enhanced properties[2]. Antigen-binding fragments, or Fabs, were the first immunoglobulin fragment-based technology to be developed and it is the most widely used, offering a set of unique properties, including reduced half-life times and enhanced tissue penetration[3]. However, in opposition to mAbs, there is no standard method of choice to capture Fabs, once there is no universal solution. Instead, a set of alternatives can be used, including affinity (e.g. protein L) and non-affinity methods (e.g. hydrophobic and ion-exchange chromatography), but all of them present limitations and drawbacks[4]. Therefore, new methods for Fab purification need to be developed, ideally for all classes of fragments and independent from the manufacturing method being used.

For the past years, phenylboronate multimodal ligand has been successfully employed to capture monoclonal antibodies, due to its affinity to cis-diol groups[5,6]. Recently, Nascimento and co-workers also showed the possibility of using this ligand to efficiently capture kappa Fab fragments[7].

The first aim of this work was to screen and optimize different variables in the papain-based antibody digestion protocol, in order to obtain a more efficient process. The variables studied included reaction time and volume, enzyme and substrate concentrations, temperature, operational pH and buffer type. The establishment of an efficient digestion protocol allowed cost and time savings, and a proper characterization of the impact of each variable on the digestion process.

The second and main aim of this work was to study the possibility of using aminophenylboronate as a universal ligand for purification of kappa and lambda classes of Fabs. For this, different chromatographic conditions were screened in a high throughput manner, using the microfluidic device previously developed by Pinto et al.[8] The screening included a set of different pH and salt concentration for binding, where also several impurities related with the fragments manufacturing process were tested - undigested antibody, Fc fragments and proteins from CHO-S supernatant - and several agents for elution, such as tris, D-sorbitol, magnesium chloride, guanidine hydrochloride, urea and arginine. These studies were complemented with the validation of results at macroscale, also allowing the extraction of additional information, as the proportion of protein bound to the column versus total protein injected and results comparison between different target molecules. The approach here used allowed the study of the interactions pattern leading to retention of target molecules in the column.

2. Introduction

2.1. Antibodies

2.1.1. What are antibodies?

Antibodies (Abs) or immunoglobulins (Ig), are a group of glycoproteins, present in the plasma and extracellular fluids, considered key players of the adaptive immune system[1]. Their main role is to recognize and bind foreign entities, with high specificity and affinity, and consequently promoting their neutralization or elimination from the body[9]. The ability of binding to different targets (molecules, proteins, carbohydrates, etc.) makes antibodies extremely flexible proteins, and so, suitable for a wide range of applications, namely in biotechnology, pharmaceutical and medical fields[1]. Abs are produced and secreted by plasma cells, a specialized type of B cells, after the binding of the receptors present in B lymphocyte's membrane to a corresponding antigen[10]. There are two ways of classifying antibodies, polyclonal antibodies (pAbs) or monoclonal antibodies (mAb). pAbs are generated when different B lymphocyte recognizes different portions of the same antigen, called epitopes, and plasma cells produce different antibodies capable of recognizing multiple epitopes from the same antigen. mAbs refers to antibodies originated from a single B cell, that are only able to bind to a single epitope from a specific antigen[1].

2.1.2. Antibody structure

Immunoglobulins are symmetrical molecules comprised of two heavy chains and two light chains, each composed by constant and variable regions, responsible for effector and Ig-Antigen binding functions, respectively[9]. According to the structure of the heavy chain, antibodies are classified into five major isotypes, including immunoglobulin M (IgM), immunoglobulin D (IgD), immunoglobulin G (IgG), immunoglobulin A (IgA) and immunoglobulin E (IgE). Regarding the light chain, there are two types, lambda (λ) and kappa (k), present in all of the five classes referred above and with similar functional properties between them[11]. Immunoglobulin G is the most abundant class of immunoglobulins, representing around 85% of the total immunoglobulins present in the human serum, and has the most wide range of applications[12]. For these reasons, this literature review will be mostly focused on IgG.

IgG molecules are Y-shaped multi-domain proteins, with a molecular weight of around 150 kDa. Each of these proteins has two identical γ heavy chains and two identical light chains, with a molecular weight of 50 and 25kDa, respectively. There are four subclasses of γ heavy chains, corresponding to four different subclasses of IgG in humans, including IgG1, IgG2, IgG3 and IgG4. Each heavy chain is composed of three constant regions (C_H1, C_H2 and C_H3) and one variable region (V_H1). Light chains have one constant region (C_L) and one variable region (V_L)[1,3,12–14]. The four polypeptide chains are linked together by several disulphide covalent bonds[13].

According to their properties, three functional antibody regions can be identified: two identical antigen-binding fragments (Fab), responsible for the interaction with the antigen, and one crystallizable region fragment (Fc), responsible for some effector functions, such as complement fixation, activation of immune cells and immunoglobulin stability[12,14–16]. Structurally, C_H2 and C_H3 domains of both heavy

chains corresponds to the Fc region, while the light chain and the C_H1 and V_H domains of the heavy chain corresponds to the Fab fragments. Within variable heavy and variable light domains, three complementarity-determining regions (CDRs), also called hypervariable regions, are responsible for the specificity and affinity for the antigen. Other regions with lower levels of variability are also present, called framework regions (Fr), having mainly structural functions[3,10,12]. Overall, these regions are present in the Fab fragments, being these considered the variable portion of every antibody. A representation of the overall structure of an IgG molecule can be observed in **Figure 1**.

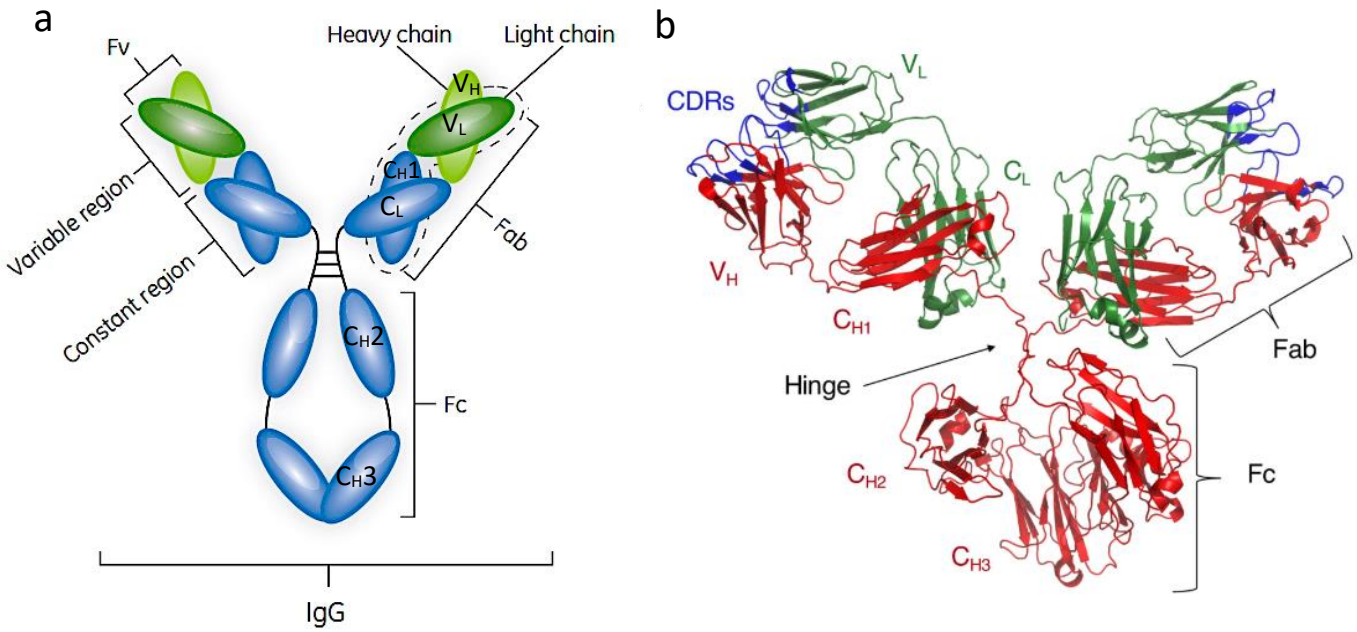

Figure 1. *Two different representations of immunoglobin G molecular structure. (a) Each IgG molecule is comprised by two similar heavy chains (C_H1, C_H2 and C_H3 and V_H1 domains) and two similar light chains (C_L and V_L domains). The IgG molecule can also be divided in two different functional regions: Fab fragment, responsible for antigen recognition, and FC fragment, responsible for effector functions. Adapted from Ref.3. (b)IgG1 structure obtained by X-ray crystallography. CDR regions of the Fab fragment, present in both V_L and V_H domains, are responsible for recognition and binding to the antigen. Adapted from Ref.9.*

2.1.3. Immunoglobulin G glycosylation

In addition to Ig structural and chemical properties, glycosylation has been shown to affect its biology activity. The presence of glycan molecules, attached to the IgG, was reported to have influence on its stability, tendency to aggregate and/or precipitate, promotion of other effector functions and, if the modification occurs in the Fab portion, influence on the interaction with the antigen[14,16,17]. Also, changes in glycosylation patterns are associated with aging[18] along with pregnancy[19], and can be observed when comparing IgG molecules from healthy individuals and subjects suffering from autoimmune diseases, as rheumatoid arthritis[20]. Thus, glycosylation is thought to have an import role in modulating IgG activity.

So far, glycosylation patterns are better identified and understood in the Fc region. In all IgG subclasses, a conserved motif consisting of an asparagine, followed by a random amino acid (except

proline) and a serine or a threonine (Asn-X-Ser/Asn-X-Thr), is present in C_H2 domains, where a N-glycan can generally be found[16,21]. Although there is a significant variation regarding the monomers composing the protein, including the presence or absence of/different contents in fucose, galactose, bisecting N-acetylglucosamine (GlcNAC) and sialic acid, this molecule has a constant core structure comprised of four GlcNAC and three mannose molecules[17,22].

These post-translational modifications are also present in the Fab portion of IgG molecules, but restricted to the variable domains, corresponding to the CDRs and framework regions in both heavy and light chain. Once again, the attachment of a N-glycan requires the existence of a conserved motif Asn-X-Ser/Asn-X-Thr, but it is highly dependent on physiological, environmental and pathological conditions[14,16]. Thus, in normal conditions, 15 to 25% of the Fab domain is estimated to be glycosylated[16]. These glycans are similar to those associated with the Fc portion, but in this case, polymers tend to be richer on mannose, sialic acid and bisecting GlcNAC[22,23], where sites of glycosylation and heterogenicity in a typical N-glycan between Fab and FC are represented.

2.2. Antibody engineering

2.2.1. Antigen fragments technologies

Although mAbs have been used as a fundamental tool in diagnostics, therapeutics and in a number of different research fields, there are some drawbacks and limitations to their utilization[24]. Since full-sized mAbs have a large molecular weight, penetration and homogenous distribution in target tissues are limited. In addition, non-specific uptake by other tissues, as well as triggering of secondary immune reactions are prone to happen. For imaging applications, for example, the prolonged half-life of mAbs can be a limiting factor[2,25]. Therefore, in the past decades, development of alternatives to mAbs has gained relevance, particularly of smaller proteins with enhanced properties[2]. Two main strategies can be used, including the dismantle of full-sized immunoglobin molecules, to obtain Fab fragments, or the use of more sophisticated protein engineering techniques, to achieve novel classes of fragments, namely single chain fragment variable (scFv), diabodies and single domain antibody fragments (dAb). Either way, at least one antigen-binding domain must be preserved, so the affinity and specificity to the antigen is not affected[26]. All these alternatives to full antibodies can be seen in **Figure 2**.

Fab fragments were the first immunoglobulin fragment-based technology to be developed and it is the most widely used today[3]. Generation of Fab fragments was firstly reported in 1956, using enzymatic cleavage, resulting in two similar fragments comprised of two variable domains of both heavy and light chain, along with one constant domain from each of them, linked by disulphide bridges[27]. Because Fabs lack the Fc region, the effector functions associated with this domain are lost[28].

scFv consists of both variable domains from heavy and light chains, linked together through a short peptide linker. Although having a molecular weight of only 25 kDa, it preserves the affinity and specificity to the antigen, which is the main reason for an increasing number of scFvs therapeutics entering in clinical development and trials[28,29]. However, the smaller size makes them less stable, more prone to degradation and easily cleared from the circulating stream. In addition, using scFvs structure, other types of fragments can be obtained, as it is the case of diabodies and scFv-Fc, consisting of two

scFv molecules bound together through complementarity regions and a scFv fused to a Fc fragment, respectively[24,29].

Finally, dAbs are composed by a variable domain from either a light or a heavy chain, corresponding to a molecular weight of 12-15 kDa, in contrast to full-sized antibody (around 150 kDa), Fabs (50 kDa) and scFv (25 kDa). Thus, they represent the smallest fraction of the immunoglobulin molecule, which retain its ability to recognize and bind to the antigen[3].

From now on, this literature review will be focused on Fab fragments.

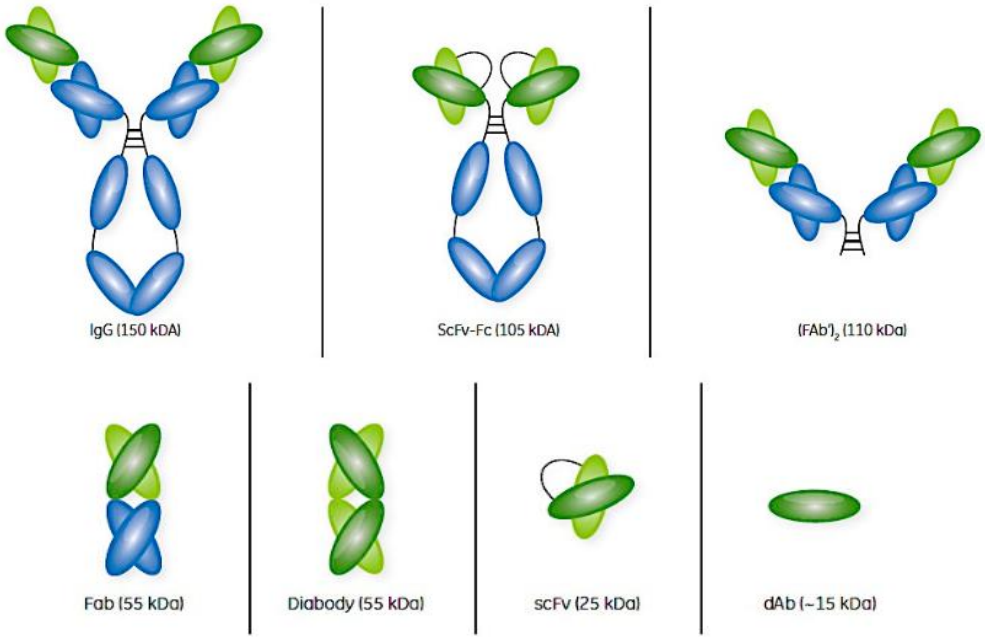

Figure 2. *IgG molecule and its molecular alternatives. There variations can be further divided in two groups: those obtained by dismantlement of the IgG molecule, either Fab or (Fab')$_2$, or those requiring more sophisticated engineering techniques, including scFv, scFv-Fc, diabodies and dAb. In all cases, except for the scFv-Fc, effector functions associated with the Fc region are lost. Edited from Ref 3.*

2.2.2. Advantages and drawbacks of Fab Fragments

Fab fragments-based technologies present a set of different properties which, when compared with the intact immunoglobulin molecule, can be beneficial or not, depending on their applications. Firstly, since they are smaller, these fragments have a better capacity for tissue and tumour penetration. However, since they lack the Fc region, these molecules are less stable, have a lower half-life, reduced tissue retention times and faster elimination from the body[24,28]. These characteristics can be beneficial for some applications, for example fast but short-termed penetration in tumours or *in vivo* imaging, but have a negative impact on applications that require long-term effects[3]. To overcome this problem, several strategies have been employed, including the coupling of polyethylene glycol (PEG)[30] or fusion to other small proteins, such as human serum albumin[31] and albumin-binding peptides[32]. Also related with the lack of the Fc region, these fragments are not able to trigger effector functions, normally ensured by the Fc domain[29]. Moreover, since they are smaller, they can be less prone to trigger immune reactions[28]. Finally, related to Fabs manufacturing, it can be carried out in prokaryotic cells, instead of

using mammalian cells. For this reason, Fab fragments production is generally less expensive, than the traditional manufacturing of entire immunoglobulin molecules[29].

2.2.3. Ranibizumab vs. Bevacizumab: a case of study

Neovascular age-related macular degeneration (AMD) is a growing eye disease that leads to the most significant number of blindness cases between older people in Europe and United States[33]. During the development of this condition, there is an unusual growth of blood vessels in the macula, part of the retina, which eventually causes leakage and subsequent swelling and formation of a scar. This later phase results in the irreversible loss of vision[34]. Indeed, development and leakage of arteries and veins are triggered by the vascular endothelial growth factor (VEGF), overexpressed in several pathologies, including AMD and colorectal cancer. Therefore, currently employed AMD treatments target VEGF to avoid these effects[33,34].

Currently, the most widely used drugs targeting this disease are ranibizumab (Lucentis®), a 49 kDa Fab fragment from a recombinant humanized mAb, and bevacizumab (Avastin®), a 149 kDa recombinant humanized mAb, both commercialized by the same pharmaceutical company, Roche[35,36]. Bevacizumab was the first to be employed with this purpose, in 2005, even though, so far this drug is only approved by Food and Drug Administration for cancer-related treatments. One year later, ranibizumab was approved in USA, by the same agency, to treat neovascular AMD, by direct ocular injection[35,37]. These alternatives are both represented in **Figure 3**.

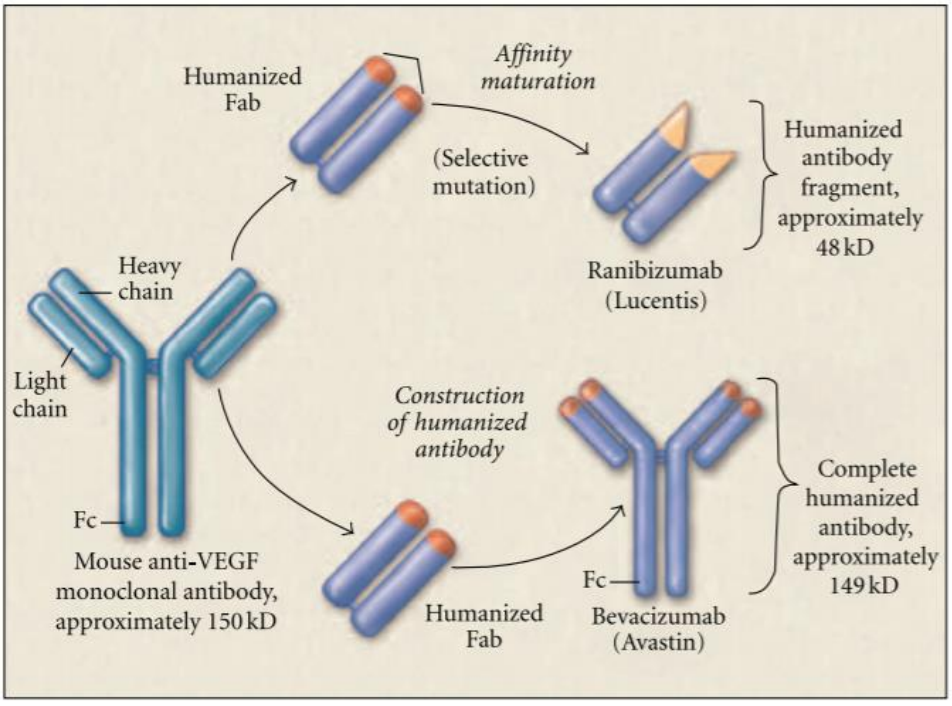

Figure 3. *Ranibizumab (Lucentis®) and Bevacizumab (Avastin®) as therapeutics for Neovascular age-related macular degeneration. Both of them are derived from a mouse anti-VEGF monoclonal antibody, but Ranibizumab is a recombinant humanized Fab fragment, while Bevacizumab is a recombinant humanized IgG molecule. Adapted from Ref.36.*

Given that the Fab fragment has a lower molecular weight, it would be expected to have a set of different properties, such as lower tendency to provoke adverse side effects, due to a quicker elimination from the human body, potential higher affinity to VEGF molecules and higher penetration rate into the target tissues[35]. However, both drugs seem to have similar clinical efficacies, except that better anatomical results are observed when using ranibizumab[33,38]. In contrast, safety studies are not consensual, since some of them show similar safety profiles, except for gastrointestinal disorders[34], while others prove worrying results concerning systemic major adverse incidents when using the full-sized mAb[38].

Nevertheless, the main factor determining the usage of one over the other is the selling price. Since bevacizumab is purchased in large amounts for colorectal cancer treatment, it costs much less than ranibizumab, only sold in a single-use format, corresponding to a retail price of 55 and 2,023 US dollars per dose, respectively. For this reason, ranibizumab represents 33% of the sales, while bevacizumab stands for the remaining 64%[35]. This case of study illustrates the real possibility of antibody fragments to replace their original immunoglobulin molecules, with focus on Fab fragments.

2.3. Fab production and downstream processing

2.3.1. Manufacturing techniques

Antigen-binding fragments can be obtained using two main strategies: traditional Ig enzymatic digestion or recombinant protein expression[39].

Regarding enzymatic cleavage, papain is the most commonly employed enzyme, used to obtain one Fc and two identical Fab fragments[40]. It starts its activity by introducing a cut between position 224, histidine, and position 225, threonine, and further breaking down of the position 233, glutamic acid-position and 234, leucine, both in the heavy chain, but eventually other non-specific cuts can be introduced[41]. Although it can fragment all IgG isotypes, papain digestion was reported to present different enzymatic kinetics and yields according to the immunoglobulin subclass used[39]. Cysteine is added to the digestion mixture as a reducing agent[40].

Later on, the alternative of producing recombinant Fab fragments directly in expression systems was developed and, nowadays, it can be accomplished using mammalian cells[42], bacteria[43], yeasts[44], insect cells[45] and transgenic plants[46]. To produce Fab fragments, one important feature must be taken in consideration: light and heavy chains are expressed individually and need to be synthesized at the same levels, so they can attach to each other through disulphide bounds, and originate the active form of the molecule. An alternative to this strategy is to express the Fab fragment as a single polypeptide, with a linker between both chains[42].

Currently, mammalian cells are the most used platform to produce therapeutic antibodies, standing for around 95% of total production[47]. Despite the high costs involved, this is the expression system that leads to the most active product, generating almost identical post-translational modifications to humans, including disulphide bound formation and glycosylation patterns. Between the different mammalian cell lines, Chinese hamster ovary (CHO) cells are the most popular, since they are relatively simple to culture in large scale, can grow in suspension and in serum-free mediums [48].

A simpler and cheaper alternative to mammalian cells is the bacteria *Escherichia coli*. Their rapid growth to high cell densities, inexpensive medium requirements and a set of genetic tools that can be easily employed for its genetic manipulation, are features that make this expression system a valuable option to produce biomolecules, including Fab fragments. The major limitation is related with the lack of machinery necessary to produce glycosylated Fabs. Nevertheless, *E. coli* is a valuable alternative to mammalian cells lines, being both Fab fragments Ranibizumab and Certolizumab pegol produced in this expression system[43].

Another possibility is the manufacturing of Fab fragments in yeasts, which combine the advantages of eukaryotic and prokaryotic recombinant systems, including: the ability of performing post-translational modifications, easy genetic manipulation, simple and inexpensive medium requirements and fast growth. Currently, *Pichia pastoris* is the most widely used species of yeast to produce Fab fragments. In spite of all these benefits, hyperglycosylation, limitated secretion of large proteins and degradation of secreted proteins represent serious obstacles to its implementation as a relevant platform to the production of therapeutic antibodies[47]

In the last years, insect cells have also been presented as a reasonable alternative to mammalian cells, because they are easier to cultivate, while performing identical post-translational modifications to humans, required for Fab correct folding and activity. Although a difference of 3 kDa between a Fab produced in Drosophila S2 cells and the Fab obtained by enzymatic digestion was reported in a study, suggesting different glycosylation patterns, the affinity to the respective antigen was the same in both cases[45].

Finally, transgenic crop plants can be cultivated to synthetize and accumulate large amounts of recombinant antibodies, using for example potatoes or tobacco species, as it is the platform with the easiest scale-up. However, differences in the glycosylation patterns, long and laborious genetic manipulation techniques and the processing of large amounts of biological materials in the downstream processing pose relevant obstacles to its implementation[46].

2.3.2. Downstream processing

2.3.2.1. Purification of mAbs

After production, antibodies molecules are submitted to complex downstream processes to eliminate impurities and contaminants, while maintaining product structural properties and biological activity. The goal of every downstream process is to ensure that the final product is pure and that the safety and quality standards are respected. Also, special caution must be taken when dealing with biopharmaceuticals produced in mammalian cells. Since the presence of virus could be extremely harmful for the patient, virus clearance steps must be considered to assure removal and inactivation of possible virus particles present in solution[4]. Since Fabs for pharmaceutical applications can be originated from full mAbs, their purification must result from an adaption of the mAbs downstream processing, considering their features. For this reason, a brief description of this process will be firstly reviewed.

After cell growth, mAb downstream processing starts with cell harvest and clarification of the cell culture supernatant, usually by centrifugation, to exclude cells and cell debris, and/or depth filtration,

to eliminate particles larger than 0.22 µm. If the desired product is not secreted, cells need to be previously lysed[4,49]. Then, the clarified supernatant is submitted to a capture step, generally performed by protein A affinity chromatography. Protein A has great affinity towards the constant domains of the Fc region of mAbs - C_H2 and C_H3 - making it a universal solution for the purification of these biomolecules. Alternatives to protein A includes other chromatographic processes such as ion exchange (IEX), multimodal (MMC), hydrophobic interaction (HIC) or other type of non-chromatographic solutions (aqueous two-phase systems, precipitation, among others). The goals of the capture step is to reduce the feedstream volume and to eliminate the main impurities[50]. In the end of the capture step, a polishing step is performed in order to remove trace amount of impurities, aggregates, possible leached ligands and specific impurities, such as host cell DNA, proteins and virus. For this, several chromatography variants can be used, including HIC, anion (AEX) and cation exchange (CEX) chromatography or size exclusion chromatography (SEC). As mentioned before, a step of viral clearance is also required, consisting in a low pH hold and in a viral filtration. Lastly, the final product is concentrated and the buffer exchanged by ultrafiltration/diafiltration, where specific components are added to create a given final formulation. A scheme of the entire process is represented in **Figure 4.**

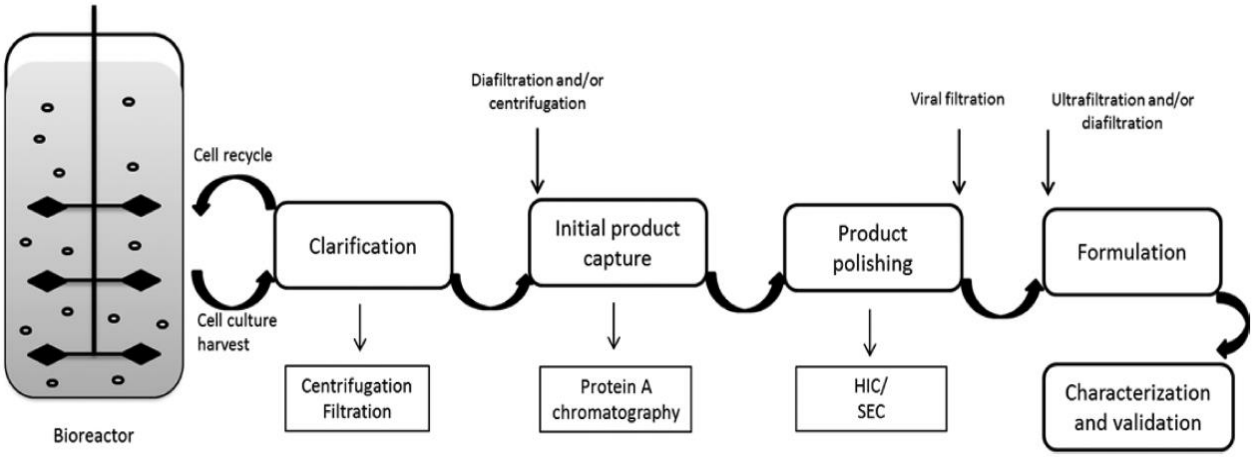

Figure 4. *Typical mAB purification processes consist in 4 steps: clarification, where cells are removed and the growth medium is clarified, a capture step, to reduce the working volume and exclude major impurities, a polishing step, to remove specific impurities and precipitates, and formulation, where specific compounds are added to the concentrated final product. If mammalian cells are used as the expression system, further viral clearance operations are required. Adapted from Ref.50.*

2.3.2.2. Purification of Fab fragments

In contrast to what happens for monoclonal antibodies, there is no standard method of choice for purifying Fabs. Instead, a set of techniques and methodologies are applied, but none of them has the strength and universality of protein A, that can be used to purify all classes of mAbs. For Fabs there is no such solution, once there is no universal affinity ligand. The techniques used to purify these biomolecules are: protein A, G and L or other alternative affinity ligands, metal-ion affinity

chromatography (IMAC) based on peptide tags and non-affinity chromatography, including IEX, HIC and SEC[4].

Protein A from *Staphylococcus aureus,* apart from the affinity to C_H2 and C_H3 present in the Fc fragment, also has some (lower) affinity to the variable heavy chain from V_H3 subclass. Thus, protein A could be used as an affinity ligand to this subclass but not as a tool for the remaining Fab classes[51]. Also, if Fabs are produced by digestion of mAbs, Protein A can be used to remove non-digested IgG molecules and Fc[39]. One alternative to protein A is the protein G, from Streptococcal species, that can also be used to bind the undigested IgG and Fc, after enzymatic cleavage of mAbs. Protein G has a high affinity towards the Fc region of mAbs and some affinity towards C_H1. However, this last is not high enough to be applied as a solution to purify Fabs and, in addition to this, this interaction does not occur in fragments derived from the IgG2 subclass[51]. The most applied solution to capture Fabs is the protein L from *Peptostreptococcus magnus*[48]. The interaction between protein L and Fab fragments occurs through the variable k light chain, and so this ligand cannot be applied for the purification of fragments containing λ light chains. Overall, none of these affinity ligands can be widely applied for every Fab downstream processing. Moreover, they are sensible to the harsh elution conditions generally used in affinity chromatography and present high purchase costs[50]. Nevertheless, and despite all drawbacks, these ligands are still used for antibody and antibody fragments purification due to a lack of efficient alternatives. The molecular structure of these proteins, along with the respective sites of interaction with antibodies, are represented in **Figure 5**. Synthetic peptide ligands are currently being developed to mimic these natural interactions with enhanced properties, presenting, for example, lower costs and higher resistance to extreme elution conditions, and may become in the future the method of choice[4,50].

For genetic engineered Fabs, other possibility is the use of affinity tags, generally fused to the protein C-terminus and cleaved after purification[39,45]. Proteins containing these tags, for example a histidine tag, are recovered by IMAC, taking advantage of the affinity of histidine to certain metal ions, such as nickel, copper and zinc ions. These interactions eventually are disrupted by adding a competing agent to the binding sites[4,52]. However, for biopharmaceutical purposes, this is also not the best option, because these tags are associated with increased tendency to aggregate and sensitivity to cleavage by cellular proteases. Plus, an additional tag cleavage step must be performed in the downstream processing and the fusion of peptide tags to recombinant proteins can lead to incorrect folding, potentially resulting in decreased affinity and specificity to the antigen[3]. All of these drawbacks represent challenges to antibody-fragments purification

Besides affinity chromatography, non-affinity-based methods are currently employed, which offer the advantage of considerably lowering the purification costs. Currently, CEX is one of the most applied solutions for the initial capture of basic Fab fragments[53]. AEX, SEC and HIC can also be used to polish Fab fragments, as it happens in the traditional mAb purification scheme[39]. The development of a traditional IEX (that could be cation or anion), or other non-affinity methods, to purify Fab fragments generally requires a study of the best binding and elution conditions to achieve an efficient purification step[39].

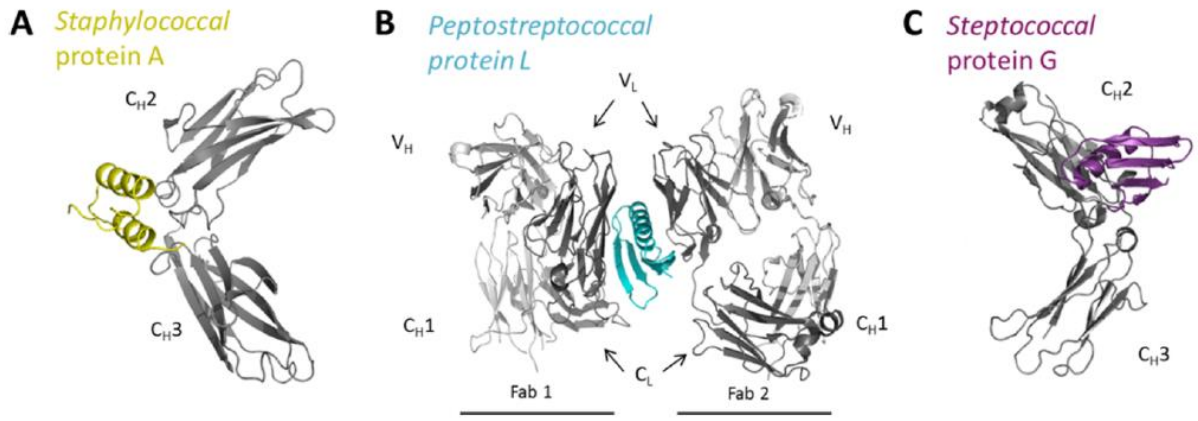

Figure 5. Sites of binding to antibodies of different affinity ligands, used for purification of mAb and respective derivates: (A) Protein A from *Staphylococcal aureus*, (B) Protein L from *Peptostreptococcus magnus* and (C) Protein G from Streptococcal species. Adapted from Ref.50.

Therefore, opposite to what happens with full-sized antibody purification, there is no preferable method for capture of Fabs. Instead, a set of techniques can be used, including affinity and non-affinity methods, each one of them presenting advantages and drawbacks. For this reason, new methods need to be developed for Fab downstream processing, which preferably must be suitable for all classes of Fabs and does not depend from the production method and the expression system used.

2.3.3. Multimodal ligand chromatography

Unlike traditional chromatography, where molecules are separated according to a single property, for example charge in IEX, size in SEC or hydrophobicity in HIC, multimodal or mixed-mode chromatography takes advantage of more than one type of interaction between the stationary phases and the solutes transported by the mobile phase[54]. This method was first employed in 1956, when hydroxyapatite was used to separate proteins, but, in the last years, this concept has gained importance, with an increasing number of publications each year[55,56]. The ability to combine different interactions modes (e.g. ion exchange, hydrophobic interaction and hydrogen bonding) in a single ligand, can improve selectivity and specificity to the target molecule when using the proper set of condtions[57]. In addition, it is also possible to use multimodal media to perform traditional chromatography, by using conditions that neutralize all interactions but one[54].

MMC media can be obtained using different strategies. The simpler strategy is to independently and uniformly add different interactions in the matrix, which are given by contiguous ligands, so they can bind to the target molecule in a multimodal way. However, the most used strategy is to add groups providing different interactions to a chemical scaffold[56].

In most of the cases, the types of interaction selected are hydrophobic (e.g. phenyl or butyl groups) and ionic, either strong (e.g. quaternary ammonium groups) or weak (e.g. carboxyl and amino

groups). Also, other types of secondary interactions have been demonstrated to play an important role on protein-ligand interaction, as is the case of hydrogen bonding and thiophilic interactions[57].

2.3.3.1. Boronic acid and its derivates

Although affinity of boronic acid [$RB(OH)_2$] to cis-diol compounds was firstly reported more than 170 years ago, the tremendous development of applications based on this interaction is recent and related with the boom of proteomics and metabolomics. These advances were driven by the development of new boronate materials, such as monoliths and nanoparticles, which present high levels of specificity and selectivity[58]. Before that, significant applications were restricted to separation of glycosylated haemoglobins and clinical diagnosis of diabetes, performed since the 70s, when immobilization of this compound in chromatography media was first achieved[59]. Nowadays, boronic acid and respective derivates are used as ligands in the so called boronate affinity chromatography, for purifying a variety of biomolecules, including carbohydrates[60], nucleic acids[61] and glycoproteins[62]. For all these applications, 3-aminophenylboronic acid (3aPBA) is the most widely used derivate[63].

Boronate affinity chromatography is based on the establishment of covalent bounds between boronic acid and cis-diol compounds, via reversible esterification reaction, which is highly dependent on environmental pH. Under acidic conditions, when the working pH is lower than boronic acid pKa (approximately 8.8-8.9 in water), the ligand adopts a trigonal coplanar configuration (sp2). When the pH is increased to values higher than the ligand pK_a, conformation is switched to a tetrahedral negatively charged form (sp3). Both configurations can bind to cis-diol compounds, but the equilibrium constant is higher in the second case, resulting in more stable complexes and slower dissociation rates at higher pH values[58,64,65]. Binding to 1,2-cis-diol molecules, where two hydroxyl groups have a coplanar configuration, results in the strongest covalent bond, even though the ligand can also interact with 1,3-cis-diol[66]. A representation of this reaction is present in **Figure 6.** When dealing with biological samples, it is not advisable to sharply increase the pH to the values required for binding, and for this reason, several boronic acid derivates have been developed, including those with additional groups (e.g. phenyl, carbonyl and sulphonyl rings). In these cases, the coupling of an electron-withdraw group causes a decrease in the pK_a and lowers the pH required for the binding step, preventing the undesirable degradation of biomolecules[67].

Nonetheless, the binding of boronic acid to cis-diol compounds is not the only interaction occurring with these compounds, as secondary interactions can also affect ligand selectivity, namely hydrophobic and ionic interactions, hydrogen bonding and Lewis base coordination[66].

Since most of these ligands are aromatic boronic acids, containing for example phenyl groups, they are prone to establish hydrophobic interactions, as well as aromatic π-π or even cation-π interactions. If it is true that these secondary interactions can increase selectivity to the ligand, it is also true that they can lead to undesirable non-specific adsorption of impurities, such as other proteins and nucleis acids[58,66]. Thus, the possibility of having hydrophobic interactions and their respective impact on the final product must be considered in a case-by-case approach. If needed, the use of alternative ligands based on hydrophilic boronate molecules or the addition of organic solvents to the mobile phase

should be considered, since these strategies were proven to exclude or minimize the occurrence of these interactions[68].

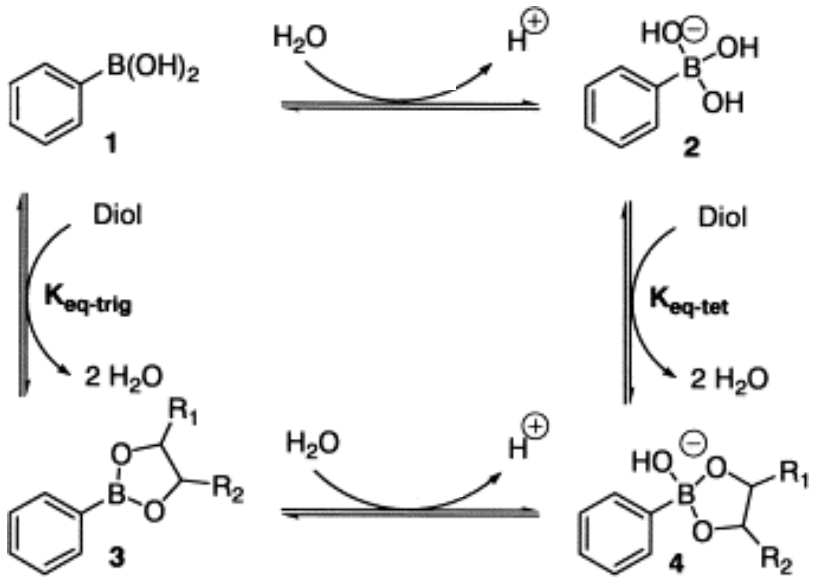

Figure 6. *Representation of the interactions happening between boronic acid and cis-diol compounds. Boronic ligands have two stable 3D configurations depending on the surrounding pH: If the pH is higher than the boronate* pK_a*, it adopts a tetrahedral configuration, while under acidic conditions, the ligand exist in the trigonal configuration. Constant equilibrium for the tetrahedral conformation is higher than for the trigonal form, making complexes more stable. Adapted from Ref.65.*

Other major secondary interaction affecting ligand selectivity is electrostatic interaction, due to the presence of the boronate negatively charged form, at binding pH values above the pKa of the ligand. Once again, the formation of these attractive or repulsive forces can increase the selectivity of the ligand, or lead to the unwanted retention of impurities according to their charges[66]. One possible strategy for disrupting these interactions is to increase the salt concentration in the mobile phase, which has to be balanced with the increase of hydrophobic interactions when higher ionic strength is applied[68]. Another solution when dealing with negatively charged compounds containing cis-diol (e.g. ribonucleotides) is the addition of pyridinium to boronate ligands, which show increased selectivity[69].

During boronate affinity chromatography, formation of hydrogen bonds was reported to have no significant impact in some cases, while being one of the strongest interactions in others, namely when working with serine containing proteins. These interactions are formed due to the presence of two or three hydroxyl groups in trigonal and tetrahedral configurations, respectively, which can behave as hydrogen bond acceptors or donnors[58]. Although no significant solutions have been found so far, urea can be added to the mobile phase to study the importance of these interactions, as it efficiently disrupts hydrogen bonds[68].

Finally, boron having an empty orbital in the boron atom while in the trigonal configuration, can behave like a Lewis acid (electron acceptor) if a Lewis base is present, acting as an electron donor. This Lewis acid-base interaction is generally beneficial since it allows the change from the trigonal to the

boronate tetrahedral configuration thus increasing equilibrium constants of ligand-target molecules complexes. The chemical representation of this mechanisms can be seen in **Figure 7**, where a fluoride ion is acting as an electron donor[68]. Also unprotonated amines and carboxyl groups can act as good Lewis bases[66].

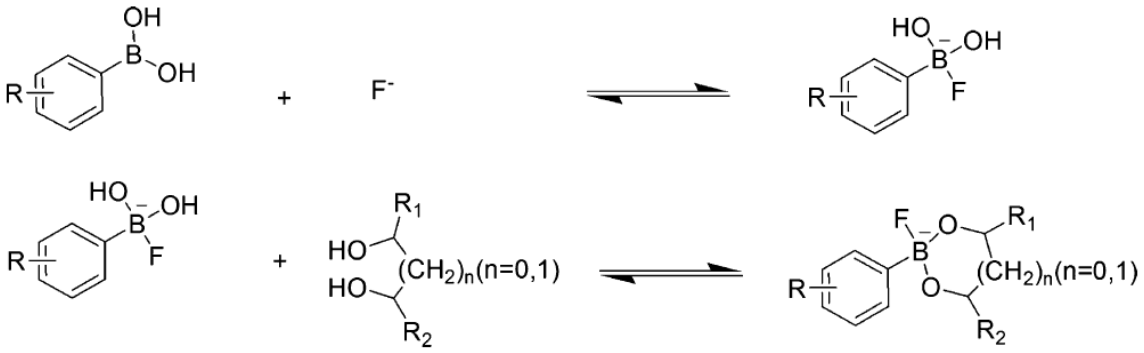

Figure 7. *Mechanism of electron transfer from a Lewis base, fluoride ion, to a Lewis acid, the boronate ligand. The ligand, when in a trigonal configuration, has an empty orbital, allowing the transfer of an electron pair from the donor to the electron receptor. After transfer, boronate ligand changes from the trigonal to a tetrahedral configuration. Adapted from Ref.68.*

2.3.3.2. Phenylboronate as a ligand for mAbs purification

As discussed before, antibodies are glycoproteins containing a well described N-glycan motif in the C_H2 domain of the Fc fragment. Although great heterogenicity can be observed regarding the terminal monomers composing this moiety, generally fucose, galactose and mannose can be found, all containing 1,2-cis-diol groups[6]. In addition, Fab fragments are exclusively glycosylated in the variable regions, but with higher contents on mannose, sialic acid and bisecting GlcNAC. These monomers also contain cis-diol groups[22,23]. For this reason, purification of both mAbs and Fab fragments is suitable to be performed using phenylboronate affinity ligands.

First studies proving the possibility of using aminophenylboronate as a tool for antibody recovery were conducted by Brena *et al.* and published in 1992. Here, proteins from human serum, including immunoglobins and complement factors, were adsorbed using 20 mM HEPES buffer pH 8.5, and eluted when switching the buffer to 0.25 M ammonium acetate pH 8.5, containing 0.2 M sorbitol. However, secondary interactions, mainly hydrophobic interactions with the aromatic groups of phenylboronate, were proven to be the driven forces acting on the process. Also, selectivity of binding was increased by adding magnesium chloride to the samples[5].

Later on, Zhang and co-workers confirmed the relevance of secondary interactions for molecules separation when using phenylboronate chromatography. In this case, binding of mAbs to the column was not affected even when N-oligosaccharides were enzymatically removed, indicating non-specific interaction of heavy chains to the ligand[70].

In 2010, Azevedo *et al.* studied the possibility of directly capture mAbs from clarified CHO cells supernatant, using phenylboronate chromatography (PBC). For this, a set of binding and elution conditions were firstly screened for IgG recovery. Among them, the type of buffer, ionic strength and pH were found to deeply affect final purity and optimized results were reached for 20 mM HEPES buffer at pH 8.5 as binding buffer and 1.5 M Tris-HCl as elution buffer. Moreover, higher purity levels could be achieved when adjusting pH of cell supernatant. Combining the optimized conditions, initial protein purity could be increased from 1.1 to 85%[6]. These results were later reviewed by Santos et al., who showed that the best results were achieved when using pH values lower than the phenylboronate pK_a. In addition, D-sorbitol was used as a competitor for elution instead of Tris-HCl, since it leads to better bioactivity levels[64].

The use of magnetic beads coated with amino phenyl boronic acid to capture human IgG was also tested by Vijaykumar *et al.*, showing promising results when applied to clarified CHO cells supernatant. During the experiments, 98% of the IgG present in solution were adsorbed to the particles, and from this percentage, 95% were successfully eluted using Tris-HCl pH 8.5 as the elution buffer[63].

Financial viability of the traditional mAb downstream processing, comprised of protein A affinity chromatography, CEX and HIC, was compared to the alternative strategy, using phenylboronic chromatography, AEX and HIC, by Grilo *et al*. This analysis proved that a cost reduction in 44% is possible if using the boronate ligand-based process. Therefore, this strategy was showed to be economically viable in theory but the switch in the process will require determination and willingness to change by the industry[71].

More recently, Rosa and co-workers studied the mechanisms leading to anti-human IL-8 (anti-IL8) monoclonal antibody (mAb) recovery using m-aminophenylboronate, by flow microcalorimetry. Their findings revealed the role of pH and salt concentrations in the process. Below the ligand pKa and in the absence of NaCl, retention of the target molecule is mainly driven by PB affinity through cis-diol esterification. However, at pH higher than 9, the ligand becomes negatively charged, and electrostatic interactions become important. When both the ligand and mAb were negatively charged, around a pH of 10, target molecules were washed out from the column, as electrostatic repulsion becomes dominant. In addition, when NaCl is added, charge transfer interactions enhance affinity interactions at pH lower than boronate pKa and electrostatic interactions were observed to be suppressed under more basic conditions. Finally, the use of different resins with similar properties to PB, suggest the importance of other secondary interactions in the process, as hydrophobic and van der Waals forces[72]. In another work from the same authors, the effect of mobile phase modulators, such as sodium fluoride (NaF), magnesium chloride ($MgCl_2$) and ammonium sulphate [$(NH_4)_2SO_4$], on anti-IL-8 adsorption to m-aminophenylboronate was studied. These compounds were observed to minimize secondary interactions with the matrix and with the phenyl group and to supress electrostatic interactions. In addition, the transfer of one pair of electrons from Mg^{2+} and NH_4^+ to boron atom and the difference in electronegativity between F^- and SO_4^{2-} with the boron anion, enhanced affinity binding to anti IL-8[73].

Besides using PBC for mAbs capture, preliminary results by Nascimento *et al.*, also showed the possibility of using this strategy to efficiently capture Fab fragments, obtained by enzymatic digestion.

For elution, the best results were reached using Tris, which is known to disrupt primary and secondary interactions. In addition, adsorption seems to be independent from both pH and salt concentration. However, the authors speculate if the establishment of primary interactions is actually relevant to the process or if only secondary interactions are responsible for the retention of Fabs in the column[7]. Further studies will be carried in this work to answer these questions and to optimize binding and elution conditions, by testing additional conditions.

2.4. Process development – high throughput approaches

When developing a new chromatography technique, or optimizing one already existing, a set of operating conditions, such as stationary phase, ligand, type of buffer, binding and elution pH and conductivity, must be screened to select the best strategy. Traditional approaches consist of testing those conditions in self-packed or commercial pre-packed lab-scale columns, generally with volume capacities of 1-5 mL. However, this strategy can be time-consuming, laborious and usually limited to prior knowledge. Moreover, large amounts of reagents and biomaterial are required and a large quantity of waste is produced, making the process considerably expensive and environmental unfriendly[74].

To overcome these limitations, four types of high throughput process development techniques are commonly applied, including: microplates batch incubation, micropipette tips and miniaturized columns and, more recently, microfluidic platforms[8,75]. These methodologies offer the possibility of testing multiple conditions in parallel using low amounts of reagents. Moreover, the availability of cheaper and less time-consuming techniques allows testing completely innovative conditions, without any kind of prior knowledge about them. However, different stationary phase layouts between micro and lab-scale columns, plays the greatest disadvantage. Overall this approach enables the preliminary parallel testing of a larger set of conditions, essential for narrowing down the options to be further tested at macro scale during process development[74–76].

2.4.1. Microlitre batch incubation

This method is generally performed in 96-well microplates, where a certain quantity of resin, usually between 20 and 200 µL, is placed in each well as a slurry. After that, the sample is added and kept in suspension for a certain period, after which, the supernatant is removed for analysis. This system allows the testing of multiple parameters in a single plate, as it can be seen in **Figure 8**, where different pH values, buffer concentrations and types of resins and buffers are being experimented. Miniaturization and parallelization are accomplished by adding a robotic liquid handler to aliquot both resin and samples into and out of the wells, with increased precision levels[77]. However, this robotic system is expensive and complex. Additionally, this method does not consider the continuous flow of the mobile phase through the stationary phase, observed in classic chromatography, and consists of only one equilibrium stage[8].

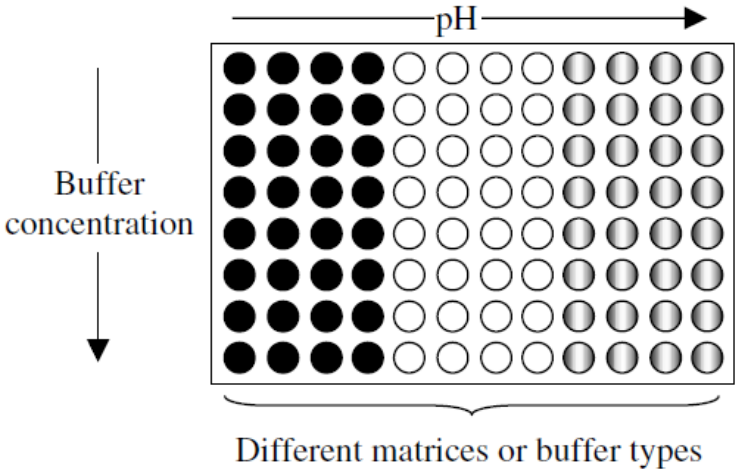

Figure 8 *Representation of a high throughput screening of several conditions, including pH, buffer concentration, resin and buffer types, using a 96-well plate. Analytes are added to the previously added resin slurry and maintained in suspension. After a certain period of time, supernatant is removed and used for analysis. Adapted from Ref:74.*

2.4.2. Micropipette tip columns

The second method is the use of a micropipette tip to mimic a chromatography column. In this case, the resin is fixed at the bottom top of the prepacked tip, which are commercialized by different companies. In opposition to the previous case, a vertical bidirectional flux is created by the repetitive up and down at a fixed flowrate, where different buffers can be used for binding and elution[78]. Once again, a robotic system can be attached to automatize the system. In any case, unidirectional and continuous flow observed in traditional chromatography cannot be truly mimicked using this system. Moreover, it works as a semi-batch process unlike lab-scale chromatography[78]. A representation of the process can be observed in **Figure 9.**

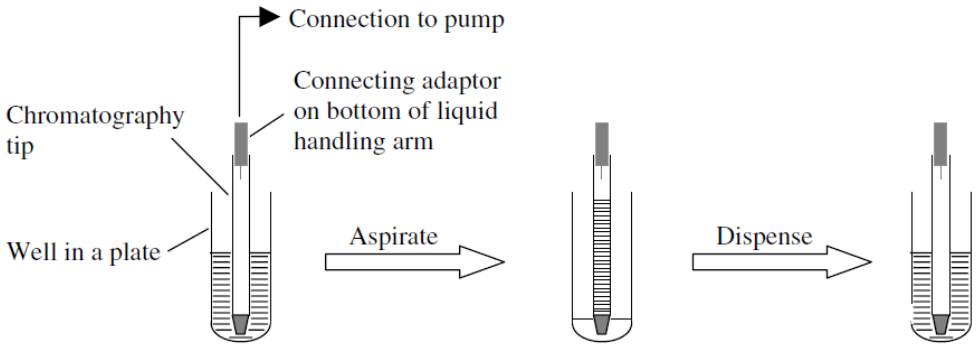

Figure 9. *Representation of an automated process based on micropipette tips columns. Resin is present at the end of the tip, in grey, and the tip is connected to a robotic arm via an adaptor. The robotic system controls the pumping of the liquid. Adapted from Ref:74.*

2.4.3. Miniaturized columns

In opposition to the previous methods, the geometry of miniaturized columns is identical to macro-scale chromatography columns, allowing unidirectional flow. Also, unlike the 96-well plate method, it enables the collection and the analysis of fractions and consequently a better understanding of impurities removal. Once again, automatization can be achieved by adding a robotic system, with increased precision and replicability levels. Prepacked columns are commercialized by different companies and generally have a resin volume between 200 to 600 µL[76,78]. For example, the company Repligen commercialize columns with different operation modes, including the centrifugal mode, where the sample is added to the top of the column and mobile phase passes through the stationary phase by applying a centrifugal force. For this, a pipette mode can be used, consisting of manual application of the sample, or a robotic mode, where the sample and buffers are applied by a robotic system, via an adaptor[74].

2.4.4. Microfluidic platforms

In the last years, the use of a microfluidic approaches to fabricate microcolumns has been gaining relevance, as an alternative to the previous methods described for high throughput process development[74]. Firstly, it excludes some of the disadvantages explained above, such as the lack of a continuous flow, high cost and complex automatization processes. Also, it offers an integrated system for experimentation and detection, while requiring even lower amounts of sample and reagents. Moreover, results are obtained faster with this approach, generally within a few minutes. One drawback is related with microfabrication, once the manufacturing process involving glass or silicon is more complex and expensive[7,8].

One representative example of this is the microfluidic platform produced by Huft and co-workers. A polydimethylsiloxane (PDMS) device was produced using a multilayer soft lithography procedure and allowed parallel and integrated experimentation of chromatographic conditions. Beads get trapped inside the 20 mm longer columns, because height of the bottom of the column is smaller than the beads diameter. Gradient of buffers can be directly prepared, using valves to control the amount of buffer A and B, mixed and saved at a storage column, before application. Different operational conditions can be assessed to a maximum of 4 columns in parallel. Eluted samples are automatically recovered for further analysis. Overall, this device offers all functionalities and respective integrated control, needed to performing chromatography experiments, including resin packing, sample injection, buffer preparation and injection and storage of eluted samples, and it was validated using a AEX resin for labelled DNA separation, based on fragments molecular weight[79].

More recently, Pinto *et al.* produced a chromatography chip for the screening of different pH values and salt concentration, for mAbs purification using a multimodal ligand. In this case, microfluidic columns were also fabricated using PDMS soft-lithography. A schematic of the chip can be found in **Figure 10**. Prior to utilization, a packing step is carried out, in which beads containing the ligand are entrapped inside the column. This is possible through a difference in height between the column

channel, with 100 µm, and the outlet channel, with 20 µm height. Since the agarose beads used had a diameter of 75-90 µm, they get mechanically trapped in the column channel, and do not flow through the outlet channel of the chip. Liquid is introduced in the system and moves towards the outlet channel, by applying a negative pressure. The effect of each tested condition on binding or elution were quantified under a microscope using fluorescence measurements of Alexa430, a photostable fluoresce probe attached to mAb molecules[8].

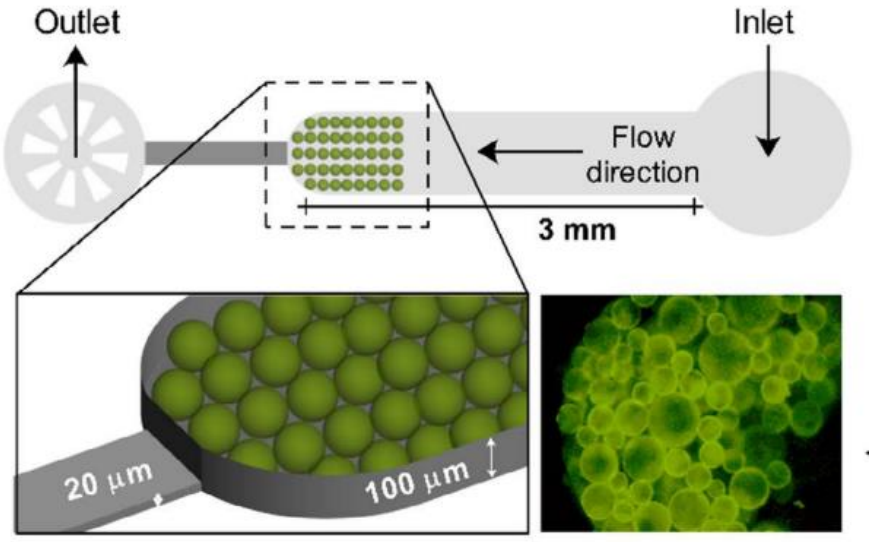

Figure 10. *Representation of the microfluidic chip produced by Pinto and co-workers for multimodal chromatography. Agarose beads (75-90 µm), containing the ligand, are trapped in the column, before entering the narrow channel (20µm). Sample and buffers are introduced in an inlet valve and move to the outlet valve, by applying a negative pressure. Coupling of a fluoresce probe to the target molecule allows quantification of binding and elution using fluorescence measurements. Adapted from Ref: 7.*

Later on, Nascimento *et al.* successfully used this platform for the screening of different binding and elution conditions of Fabs, including pH and conductivities. Two cation exchange and two multimodal ligands were tested, including phenylboronate, which was from all the options, the ligand showing the best results[7]. However, these studies were only performed for Fab fragments, containing kappa light chain.

3. Materials and Methods

3.1. Chemicals and Biologics

Human polyclonal antibody mixture, commercially named Gammanorm®, was obtained from Octapharma (Lachen, Switzerland), with a concentration of 165 mg/mL and 95% IgG (59% IgG1; 36% IgG2; 4,9% IgG3; 0,5% IgG4 and at maximum 82.5 µg/mL of IgGA). To label the IgG, BODIPY™ TMR NHS from Lumiprobe was dissolved in DMSO (Merck, Germany) and stored at minus 20ºC. CHO-S supernatant, grown in Freestyle™ CHO expression medium (Termo Fisher Scientific, USA), was kindly provided by Marta Carvalho from SCERG-iBB research group.

Tris (hydroxymethyl)aminomethane (Tris), sodium chloride, phosphate buffered saline (PBS), citric acid, D-sorbitol, EDTA, L-cysteine, iodoacetamide, papain, ammonium persulphate (APS), N,N,N,N-tetramethylethylenediamine (TEMED), glycine, sodium thiosulphate, sodium carbonate, glutaraldehyde, 30% acrylamide/bisacrylamide-solution, sodium carbonate, sodium bicarbonate, CHES, EPPS, urea and magnesium chloride were obtained from Sigma Aldrich (USA). SDS micropellets (sodiumdodecyl sulphate), 2x Laemmli sample buffer and Precision Plus Protein™ Dual Color Standards were acquired from BIO-RAD (USA), Blue safe from NZYtech (Portugal), isoelectric focusing (IEF) kit and marker from GE Healthcare (USA), trichloroacetic acid, dodecyl sulphate sodium salt (SDS), silver nitrate and formaldehyde from Merck and acetic acid from Fisher Chemical (USA). Formaldehyde solutions, sodium acetate 3-hydrate, disodium hydrogen phosphate and sodium dihydrogen phosphate were purchased from AppliChem PanReac. Also, L-arginine was acquired from ACROS organics (USA) and guanidine hydrochloride from Invitrogen (USA).

3.2. Chromatographic columns and filtration devices

Pre-packed 5 mL and 1 mL HiTrap™ Protein L and HiTrap™ Protein A HP were obtained from GE Healthcare, PA Immuno-Detection sensor cartridge from Applied Biosystems (USA) and aminophenylboronate P6XL resin from Prometic Bioseparations (Canada). Amicon® Ultra-4 centrifugal filter units (MWCO 10, 30 and 100 kDa) used for diafiltration were purchased from Merck Millipore.

3.3. Labelling of target molecules

To label IgG with the fluorophore BODIPY™ TMR NHS (with maximum excitation at wavelength of 545 nm and an emission wavelength of 570 nm), a protocol from Pinto et al. was followed[8]. Firstly, the antibody was diluted from a concentration of 165 mg/mL to 20 mg/mL, using 0.1 M sodium bicarbonate buffer pH 8.3-8.5. The dye is added at a BODIPY:IgG volume ratio of 20:1 and the mixture is incubated in the dark under mild agitation for 4 hours, at room temperature. To remove the free unreacted dye, final solution is diafiltrated with PBS using Amicon Ultra-4 centrifugal filter units (MWCO of 100 kDa) and centrifuged at 3,000g for 10 minutes. The degree of labelling (DOL) was calculated for labelled proteins as described by Pinto et al.[80], and according to the following equation:

$$DOL = \frac{(\text{A545 x MW})}{1.4 \text{ x } (\text{A280} - \text{A545 x CF}) \text{ x } \varepsilon\text{dye}}$$ **(Equation 1)**

Where A_{545} represent the absorbance of labelled proteins at 545 nm, the maximum excitation wavelength of BODIPY™ TMR NHS, MW corresponds to protein molecular weight, A_{280} is the absorbance of the conjugate at 280 nm, CF is the contribution of the dye in A_{280}, and ε_{dye} is the extinction coefficient of the dye at 545 nm. For BODIPY™ TMR NHS, CF is 0.16 and ε_{dye} is 60,000 L/mol/cm[81].

3.4. Antibody digestion

The digestion protocol herein applied was based on the work of Andrew et al[40].

First, for screening of the factors relevant in the digestion process, the digestion time was varied (0, 2, 4, 6, 8, 10, 12, 18, 24 hours) and, for each digestion time, four different papain concentrations were used (0.2; 0.1; 0.05; 0.01 mg papain/mL). The remaining parameters, namely volume, IgG concentration and buffer composition, were maintained as standard conditions in every experiment using this strategy (500 µL; 1 mg IgG/mL; PBS pH 7.4, respectively), except when indicated. Then, for 6 hours of digestion and 0.1 mg papain/mL, different reaction volumes were tested (1, 2 and 5 mL), and for each of them, different IgG concentrations were used (1, 2, 5 and 10 mg IgG/mL). Also, several buffers combined with different pH values were tested: 10 mM phosphate buffer pH 6.5, 7 and 7.5, 10 mM Tris buffer 7.5, 8, and 8.5 and 10 mM Tris buffer 150 mM NaCl pH 8, for 6 hours digestion, 1 mL final volume, 0.1 mg papain/mL and 1 mg IgG/mL. Finally, also using these conditions, different temperatures were tested (25, 37 and 40ºC).

For the DOE approach, two parameters were changed at a time, including temperature (25, 33 or 40ºC), digestion time (1, 12.5 or 24 hours), papain concentration (0.01, 0.105 or 0.2 mg/mL) and Gammanorm® concentration (1, 5.5 or 10 mg/mL).

In all experiments, EDTA and L-cysteine were kept to a final concentration of 0.015 M. To stop the reaction, a solution of 0.3 M of iodoacetamide was added to a final concentration of 0.03 M.

The design of experiment (DOE), along with the treatment of multivariable data was performed using MODDE Go software, developed and commercialization by Umetrics. Data was adjusted to a multiple linear regression. D-optimal model was used for DOE.

3.5. Chromatographic runs

Chromagraphic experiments were performed using ÄKTA™ Purifier 10 system (GE Healthcare), which allowed conductivity, pH and UV absorbance at 280 nm continuous monitoring. All the data was acquired by the software Unicorn 5.1 and fractions were collected using a Fraction Collector Frac-950 from GE Healthcare.

3.5.1. Quantification of antibody digestion

After digestion, Fab fragments were indirectly quantified using an analytical protein A quantitative column, PA Immuno-Detection sensor cartridge, as performed by Nascimento and co-workers[7]. 50 mM phosphate 150 mM NaCl pH 7.4 and 12 mM HCl 150 mM NaCl pH 2.3 were used as adsorption and elution buffers, respectively. Concentration of each sample was calculated considering a calibration curve, drawn from results obtained for samples ranging from 0.005 to 1000 mg IgG/mL. Efficiency of digestion was calculated based on the reduction of the elution peak, assuming that 100% of digestion correspond to a 67% reduction, as in this case only Fc fragments bind to column and two Fab fragments are produced from each antibody digested.

3.5.2. Downstream processing of Fab fragments

After the enzymatic cleavage of the labelled IgG, the digestion mixture was submitted to a purification protocol developed by Nascimento et al., 2018[7], with the aim of obtaining purified kappa and lambda Fabs and Fc fragments. This consisted in a protein A, followed by a protein L affinity chromatography, using PBS pH 7.4 (0.01 M phosphate buffer, 0.0027 M potassium chloride and 0.137 M sodium chloride) and 0.1 M citrate buffer pH 2.5, as binding and elution buffers, respectively. In both cases, flow-through and elution fractions were collected and neutralized by adding 2 M Tris pH 9. Diafiltration steps were performed to concentrate and further purify the samples. For this, Amicon Ultra-4 centrifugal filter unites (MWCO of 30kDa) were used in all the cases, but for protein A elution fractions, a 100 kDa MWCO membrane was previously used to exclude undigested IgG molecules.

Protein concentration was determined by reading samples absorbance at 280 nm and using a calibration curve drawn with well-defined concentrations of Gammanorm® IgG, ranging from 10 to 1000 mg/mL.

3.6. Fabrication of the microfluidic device

The microfluidic structure here used for the high throughput screening of chromatographic conditions was developed by Pinto and co-workers[80] and so, the corresponding mold was already available. First, PDMS is added to the curing agent to a 10:1 weight ratio, both purchased as a SLYGARD™ 184 Silicone Elastomer Kit (Dow Chemical Company, USA). These components are stirred until a homogeneous mixture is obtained and placed inside a desiccator for around 40 minutes, under vacuum. The PDMS is then poured to a petri dish containing the mold and cured for about 90 minutes at 60-70ºC. After becoming solid, the structure is shaped with a scalper and removed from the petri dish using a tweezer. Then, the inlet and outlet are manually punched using a larger blunt 20-gauge needle and a thinner blunt 18-gauge needle, respectively, and extremities are removed so that it can fit in a microscope slide. The last is then consecutively washed in IPA, acetone and Milli-Q water, inserted in a 50 mL falcon full of Alconox solution and sonicated for at least 10 minutes. Both slides and PDMS pieces are washed with Milli-Q water and dried using compressed air. Finally, the structures are sealed against the microscope slides, by oxidizing PDMS surfaces for 60 seconds, using an oxygen plasma cleaner at the medium power settings.

3.7. Packing and outline of microfluidic experiments

The protocol used was based on the work of Pinto and co-workers[80]. The methodology used is comprised of 3 consecutive steps: packing of the beads containing the ligand, equilibration and flow of the solution containing the target molecule. In the case of elution studies, an additional step consisting in flowing the elution buffer through the column is added. First, aminophenylboronate P6XL, purchase as a slurry, is diluted in 33% (v/v) PEG 8000, to a final bead volume of 1-2%. After homogenization, a tip containing 30-50 µL of solution is introduced in the inlet and beads are packed by applying a negative pressure from the outlet using a NE-1200 programmable syringe pump (New Era Pump Systems Inc, USA). Then, beads are washed with 70 µL of the adsorption buffer to be studied. Under an inverted fluorescence microscope (Olympus CKX41) coupled to a CCD colour camera (Olympus XC30), 30 µL of a solution containing the target molecule at 60 µg/mL is flowed through the microfluidic channel, allowing monitoring of labelled proteins, as they bind to the column. Images were acquired using an exposure time and a gain of 1 second and 0 dB, respectively. Fluorescence data was extracted from three representative beads using Image J software. All experiments were performed at a flow-rate of 15 µL/min. For elution studies, 50 mM phosphate no salt was used as adsorption buffer.

OriginLab software was used to calculate F_{max} for each adsorption condition, by adjusting results to an equation based on the Hill enzymatic kinetics model:

$$F = \frac{F_{max} \times (t)^n}{(t_{0.5})^n + (t)^n} \quad \textbf{(Equation 2)}$$

where F represents fluorescence of the beads, F_{max} is the maximum rate of reaction, t is the time, $t_{0.5}$ is the time that originates half of the F_{max} and n is the dimensionless Hill coefficient.

Origin software was also used to draw heatmaps for each target molecule. To compare elution results, slopes for the first 15 seconds were determined.

3.8. Validation of the results at macroscale

A 1 mL column was manually packed with aminophenylboronate P6XL resin. All buffers were flowed into the column at a flow-rate of 1 mL/min. An equilibration step was always performed prior to injection, consisting in the addition of 10 column volumes (CV) of adsorption buffer. For all chromatographic runs, 200 µL solution containing 1 mg/mL of target molecule was injected.

For the binding studies, the column was equilibrated with the binding buffer for 5 CV. After sample injection, the injection loop was emptied with 1 CV and the column was washed with 7 CV of binding buffer. Once washed, elution step with 1 M Tris-HCl, pH 8.5 was applied, using a step or a linear gradient.

For the step gradient elution studies, the previous protocol was applied. 50 mM phosphate was the binding buffer and different concentrations of Tris, sorbitol and arginine at pH 8.5 were used as elution buffers for 5 CV. After elution, the column was stripped with 5 CV of 1 M Tris pH 8.5 to remove any molecules still attached to the ligand, and regenerated with 5 CV of 1 M NaOH. In the case of

gradient elution studies, the only difference was the application of a 10 CV gradient elution step and hold for 5 CV at 100% of elution buffer.

3.9. Characterization of target molecules

3.9.1. Protein gel electrophoresis

Throughout the experiments, SDS-PAGE was performed to determine the composition and purity of the different streams generated, including the flow-through (FT) and elution (E) pools from Protein A, Protein L and aminophenylboronate chromatography, following a protocol available in the laboratory.

First, 25 µL of sample were added to 25 µL of 2x Laemmli sample buffer and boiled for 10 minutes at 80ºC. Then, 20 µL of the previous mixture was applied into a 12% acrylamide gel and ran at 90 mV for about two hours, using a running buffer, comprised of 25 mM Tris-HCl, 0.192 M glycine and 0.1% SDS at pH 8.3. Also, 1 µL of Precision Plus Protein™ Dual Color Standards (BIO-RAD) was applied as a molecular weight marker. For visualization of protein bands, gels were stained with BlueSafe and further washed in Milli-Q water for about 30 minutes to enhance the contrast. Finally, the gel was scanned using the Bio-Rad GS-800TM calibrated densitometer. For samples containing lower amounts of proteins, a silver staining protocol was used, which offers increased sensibility. It starts by washing the gel in 30% ethanol for 10 minutes, then washing it twice in Milli-Q water for 10 minutes and proceed to a sensitization step, using a 0.02% sodium thiosulfate solution, for 10 minutes. Then, the gel is washed three times in Milli-Q water for 30 seconds and stained with a 0.15% silver nitrate solution for 30 minutes. Prior to the development step using a 3% sodium carbonate and 0.05% formaldehyde, the gel is quickly washed with Milli-Q water for one minute. Finally, a 5% acetic acid solution is poured to stop the reaction.

3.9.2. Isoelectric focusing

The isoelectric point (pI) of labelled and non-labelled Gammanorm® IgG, proteins from CHO-S supernatant, Fc and Fabs fragments was determined by isoelectric focusing (IEF), following the protocol used in Pinto et al., 2015[82].

For this technique, 3 µL of each sample were applied in a PhastGel® IEF 3-9 with 50x46x0.45 mm, along with 1 µL of a Broad IEP Kit, pH 3-10 from GE Healthcare, containing a set of components with well-defined isoelectric points. In the case of undigested antibody, only 1 µL was applied. Pharmacia PhastSystem Separation (Amersham Biosciences) was used to apply the voltage. Each run took around 30 minutes at 500 Vh.

After that, a silver staining protocol was performed, starting with a fixation step, consisting in submerging the gel in a 20% (w/v) trichloroacetic acid solution, for 5 min at 20°C. This was followed by two washing steps using a 50% (v/v) ethanol, 10% (v/v) acetic acid solution, for 2 min at 50°C, and a 10% (v/v) ethanol, 5% (v/v) acetic acid solution, for 6 min at 50°C. Then, an incubation step is performed,

by adding a 8.3% glutaraldehyde solution, for 6 min at 50°C. Again, two washing steps were carried out: 10% (v/v) ethanol, 5% (v/v) acetic acid solution, for 8 min at 50°C, and Milli-Q water, for 4 minutes at 50°C. Next, the key incubation step in a 0.5% (w/v) silver nitrate solution is executed, for 10 min at 40°C, succeeded by a washing step with Milli-Q water, for 1 min at 30°C. Finally, the development was performed with 0.015% formaldehyde in 2.5% sodium carbonate, at 30°C, until the protein bands start to appear. This reaction is stopped by adding a 5% (v/v) acetic acid solution, for 5 min at 50°C. The gel was scanned using the Bio-Rad GS-800TM calibrated densitometer.

4. Results and Discussion

4.1. Screening and Optimization of Gammanorm® digestion

4.1.1. Preliminary screening by changing one factor at a time

The first objective of this work was to screen and optimize the digestion reaction of Gammanorm® polyclonal antibody mixture. To narrow down the number of studied factors in further experiments, a first screening of several variables thought to affect IgG digestion was carried out, by changing one factor at a time. This included reaction time, reaction volume, IgG and papain concentrations, temperature and pH, in a total of 6 different parameters. After enzymatic cleavage, digestion efficiency was calculated by the amount of undigested immunoglobulin present in the digestion mixture, quantified using an analytical protein A column. At time zero, antibody molecules are intact, corresponding to the maximum absorbance elution area. On the other hand, after digestion, only Fc fragments will bind to the column. Since each antibody has one Fc and two Fab fragments, with similar molecular weights, if all immunoglobulin molecules are digested (100% digestion), then a 67% reduction in the elution peak area is expected. The results can be observed in **Figure 11**.

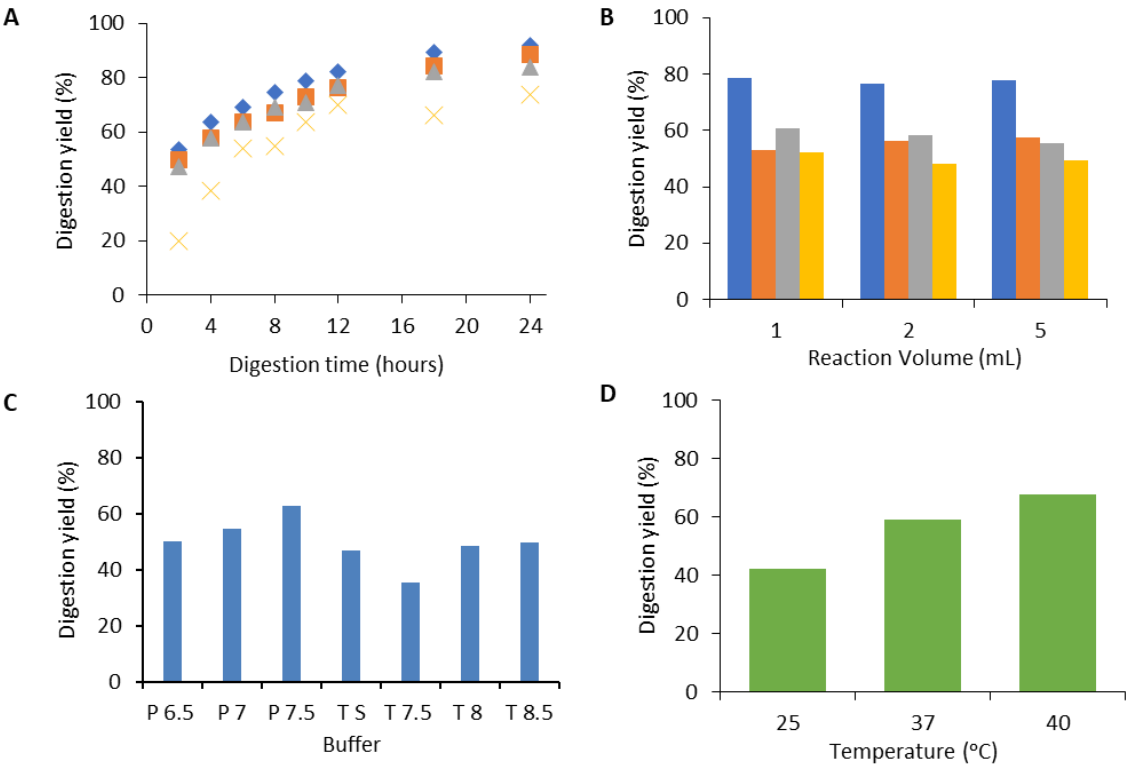

Figure 11. Impact of several factors on IgG digestion (%): **(A).** Digestion time (hours) and papain concentration (mg/mL). Blue: 0.2 mg papain/mL; Orange: 0.1 mg papain/mL; grey: 0.05 mg papain/mL; yellow: 0.01 mg papain/mL; **(B)**. Reaction volume (mL) and IgG concentration (mg/mL). Blue: 1 mg IgG/mL; Orange: 2 mg IgG/mL; Grey: 5 mg IgG/mL; Yellow: 10 mg IgG/mL **(C)**. Buffer type and pH values. P 6.5, 7 and 7.5: 10 mM phosphate buffer pH 6.5, 7 and 7.5, respectively; T S: 10 mM Tris buffer 100 mM NaCl pH 8; T 7.5, 8 and 8.5: 10 mM Tris buffer pH 7.5, 8 and 8.5, respectively. **(D)**. Temperature (ºC). The following standard conditions were used, except when indicated: 0.1 mg papain/mL, 6 hours of digestion, 1 mg IgG/mL, 1 mL total volume, 0.01 M phosphate buffer pH 7.4, 37ºC.

The first digestion parameters studied were digestion time and papain concentration (**Figure 11 A**). In three of four concentrations tested, nearly 50% of the immunoglobulin molecules were digested during the first two hours and, after that, a less significant increase in antibody cleavage is observed over time. Results were similar between all papain concentrations, except 0.01 mg/mL, which was significantly less efficient, compared with the other concentrations used. Then, different reaction volumes and IgG concentrations were tested (**Figure 11 B**). In this case, higher digestion yields were obtained for lower IgG concentrations, possibly caused by enzyme saturation, while no significant differences could be seen for different reaction volumes. No clear correlation could be stablished when testing different buffer types and pH values (**Figure 11 C**). Finally, the impact of temperature on IgG cleavage was also tested, which showed that higher temperatures lead to higher digestion yields (**Figure 11 D**).

Since the effect of some of the factors was not clear, MODDE software was used to treat the data, which allowed the development of a model describing IgG digestion in function of these variables. The model obtained had R^2 and Q^2 values of 0.757 and 0.684, respectively. The impact of each factor on IgG cleavage was further analysed and led to the exclusion of reaction volumes and pH, once they were not being relevant to define final response (**Figure 12**). On the other hand, as discussed before, digestion time, temperature and papain concentration were shown to positively influence the enzymatic reaction, while antibody concentration has a negative impact on it.

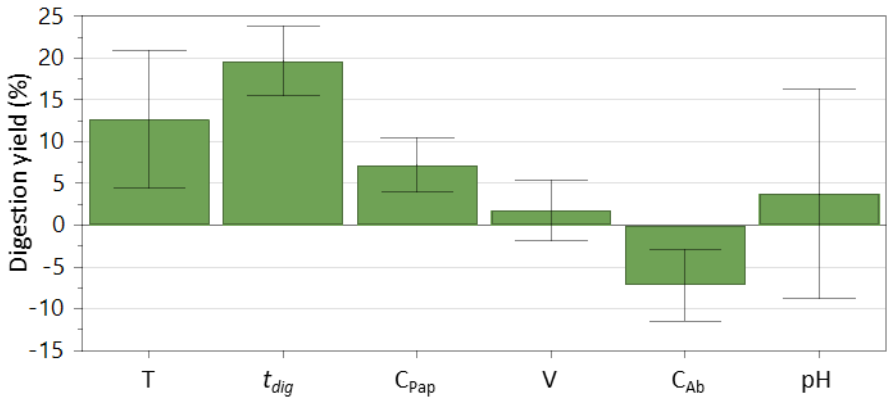

Figure 12. Coefficients (scaled and centred) for the model describing Gammanorm® digestion in function of temperature (T; ºC), digestion time (t_{dig}; hours), papain (C_{pap}; mg/mL) and Gammanorm® (C_{Ab}; mg/mL) concentrations, volume (V; mL) and pH. Results were obtained by changing one parameter at a time and by quantifying the undigested antibody present in the digestion mixture after reaction.

Samples from distinct digestion times were also analysed by SDS-PAGE (**Figure 13**). It is possible to access the dependency on digestion time by analysing the antibody band (150 kDa). This fades away along with the digestion time. The presence of Fc and Fab fragments, around 50 kDa, is well noted when digestion starts. These bands appear just after 2 hours of digestion, starting to fade over time, probably because of overdigestion. The fragments below the 37 kDa band represent both papain (23 kDa) and free light chains, produced during the reaction.

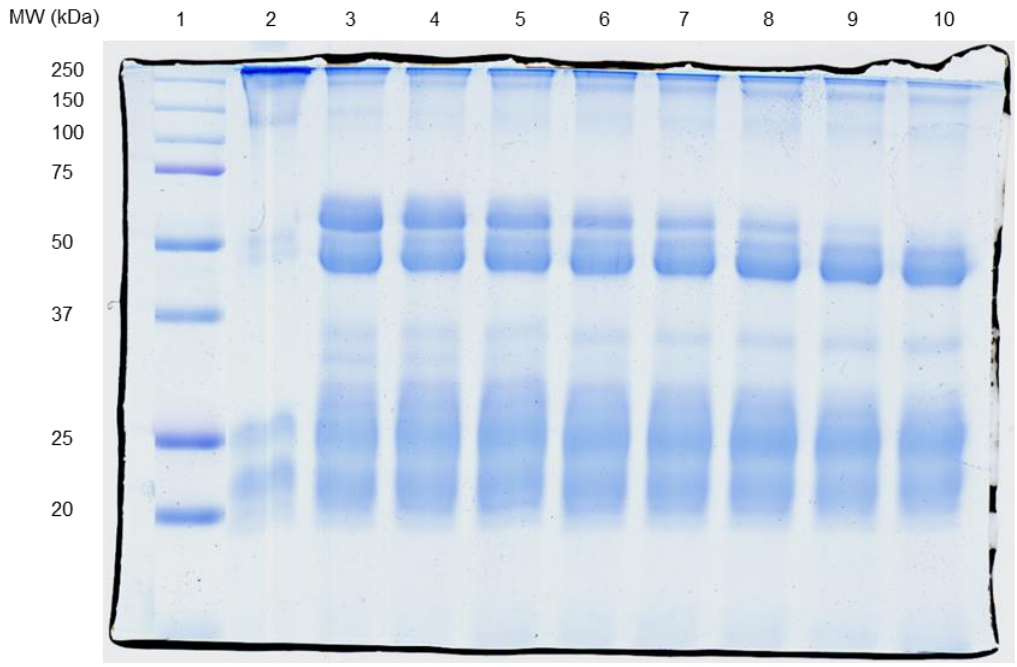

Figure 13. SDS-PAGE protein analysis of IgG cleavage mixtures with increasing digestion times. **1** - molecular weight ladder. **2** to **10** - consecutively higher digestion times: 0, 2, 4, 6, 8, 10, 12, 18 and 24 reaction hours, respectively. Remaining conditions used were: 1 mg IgG/mL, 0.2 mg papain/mL, 1 mL total volume, 0.01 M phosphate buffer pH 7.4, 37ºC.

4.1.2. Design of experiments (DOE) approach

Based on the previous results, a DOE approach was used to conduct the experiments, which allows the reduction of the number of experiments needed to extract a large set of data, by changing two factors at a time. Since variables are being shifted simultaneously, this approach allows the better understanding of critical parameters and co-dependencies. For example, for high temperature values, the optimum amount of papain is probably higher, since some of the enzyme molecules may lose their activity[83]. Therefore, a total number of 18 experiments were designed using MODDE software. After performing these trials, data was processed by the same software and used to develop another model describing antibody cleavage in function of digestion time, substrate and enzyme concentrations and temperature. The model obtained presents a R^2 and Q^2 values of 0.92 a 0.82, respectively, corresponding to a robust model. The first parameter (R^2) is representative of the model fit and reflects the differences observed between the data and the predicted response by the model and should present values higher than 0.75. On the other hand, the predictive power of the model is given by Q^2 and it is high above the minimum acceptable value of 0.5. This means the response is being accurately predicted by the model as a function of the factors[84]. The impact of each factor on digestion yield can be observed in **Figure 14**, which shows that results are similar to those obtained before, but in this case, papain concentration is the most important factor positively influencing the response, followed by temperature and digestion time. Moreover, substrate concentration has a negative impact on it, but less relevant than

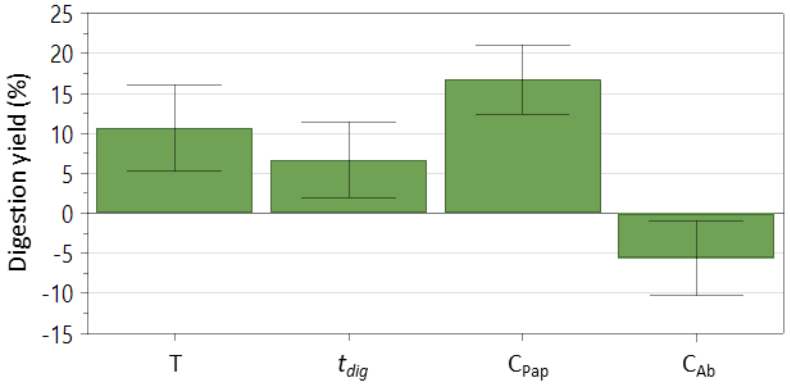

Figure 14. Coefficients (scaled and centred) for the model describing Gammanorm® digestion in function of temperature (T; ºC), digestion time (t_{dig}; hours), papain (C_{pap}; mg/mL) and Gammanorm® (C_{Ab}; mg/mL). Results were obtained by changing one parameter at a time and quantifying the undigested antibody present in the digestion mixture after reaction. A DOE approach was used to design the trials.

initial foreseen from previous results, since the corresponding uncertainty range almost crosses the yy axis.

Lastly, the optimizer tool was used to predict the optimum conditions for antibody enzymatic cleavage, which theoretically would lead to 92% digestion. Using the values presented in **Table 1**, 95% cleavage was achieved, representing a 41% increase, compared to the initial conditions.

Table 1. Optimum values of several factors, including temperature (ºC), digestion time (hours), papain and IgG concentrations (mg/mL) and their contribution to antibody digestion. Results obtained using MODDE software.

Factor	***Value***	***Factor Contribution (%)***
Temperature (ºC)	*40*	*27*
Digestion time (hours)	*24*	*17*
Papain Concentration (mg/mL)	*0.2*	*42*
IgG Concentration (mg/mL)	*1*	*14*

Overall, the presented DOE approach allowed the extraction of a large set of information from a minimal number of experiments, saving resources in the process. As mentioned in the introduction chapter, kinetics and yields of enzymatic digestion vary according to the immunoglobulin subclass being used, and consequently this protocol should be tested and adapted when working with other types of antibodies. However, since the antibody mixture used for this optimization studied - Gammanorm® - has a polyclonal nature, the protocol herein described could be seen as a suitable initial step in the implementation of a papain-based digestion protocol. Additionally, using the optimizer tool, the digestion yield could be increased for almost the double value obtained in initial experiments, saving costly

resources involved in the immunoglobulin cleavage process. In the future, using the same strategy it would be interesting to study the impact of other factors on digestion yield, such as cysteine and EDTA concentrations, used as activating and stabilizing agents[40].

However, optimum conditions may not always be the most appropriate. For example, when using higher papain concentrations or longer digestion times, undesirable over digestion can happen, due to the introduction of non-specific cuts in the immunoglobin molecules. In addition, high temperatures can cause proteins denaturation, making them unusable. For these reasons, digestion conditions must be always considered in a case-by-case approach and may not correspond to the optimum scenario.

4.2. Downstream Processing and Characterization of Fab fragments

To obtain isolated labelled fragments for the following experiments, based on a microfluidic device, the Gammanorm® antibody mixture was labelled with BODIPY™ TMR NHS, digested using the previously optimized protocol and, finally, summited to a downstream protocol. This step is comprised of two consecutive chromatographic affinity steps – Protein A and Protein L - and led to the fractionation of lambda Fabs, kappa Fabs and Fc fragments. A representation of the whole process can be observed in **Figure 15**. Flow-through and elution samples from both affinity processes, were further analysed by SDS-PAGE (**Figure 16**). Since protein A has affinity to the Fc fragment, the elution fraction (lane 4) contains different whole IgG molecules - different isotypes (two bands in the top part of the gel), Fc fragments (a band around 50 kDa) and other small digested fragments, which retained its affinity to the protein A ligand (a band around 25 kDa). The flow-through fraction (lane 3), containing kappa and

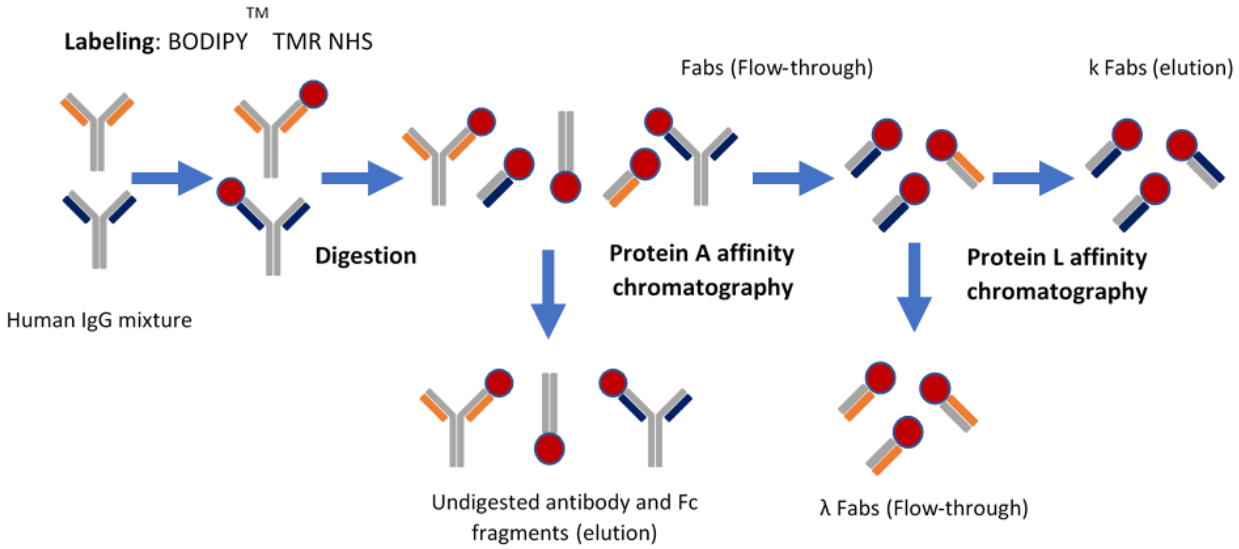

Figure 15. Protocol used to obtain labelled isolated Gammanorm® derived fragments. First, labelling of Gammanorm® antibody mixture is performed and it is followed by its digestion. After that, a downstream protocol is applied consisting of two consecutive chromatography affinity steps- Protein A, with affinity to the Fc, and Protein L, with affinity to the kappa light chains. Each fragment is recovered in a different fraction: Fc in the protein A elution, kappa Fabs in the protein L elution and lambda Fabs in the protein L flow-through.

lambda Fabs and other components from the digestion mixture, is injected to a protein L-affinity chromatography. This ligand has affinity to Fabs containing a k light chains, but not to those containing lambda light chain. As a consequence, in the elution (lane 6) kappa Fabs from different isotypes of IgG (a band around 50 kDa) and other digested fragments with affinity to protein L are present (a band below 25 kDa), for example, free light chains. In Protein L flow-through (sample 5), lambda Fabs (a fade band around 50 kDa), other digested fragments without affinity to neither protein A or protein L, along with compounds from the digestion mixture, including papain (around 23 kDa), can be found.

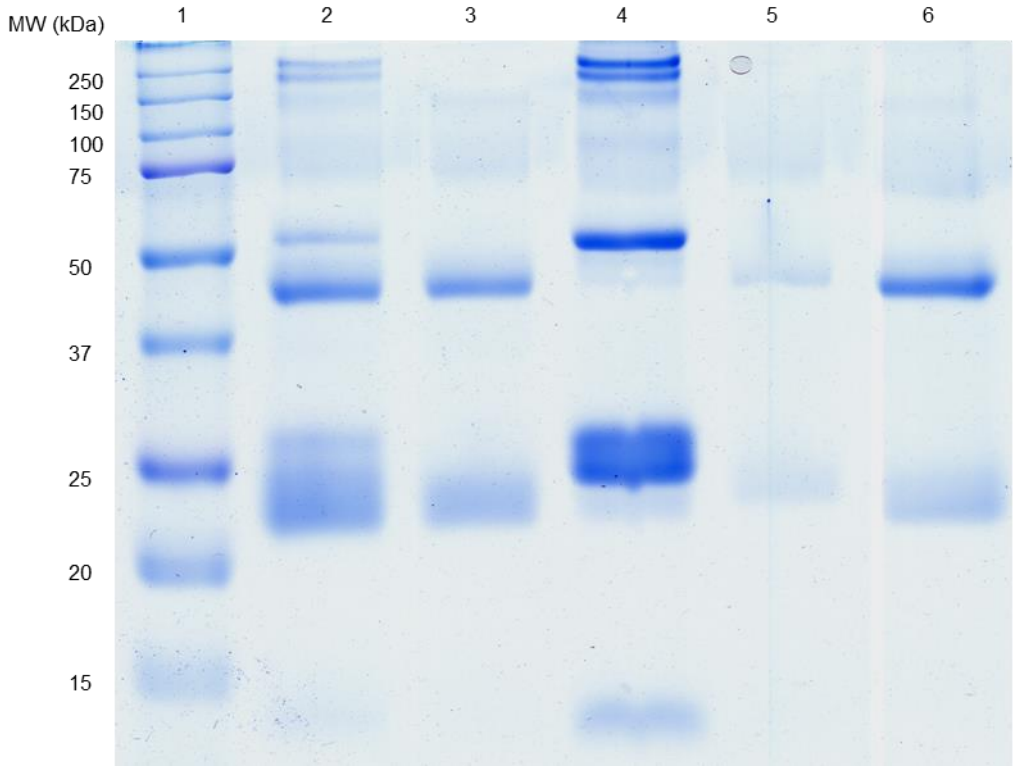

Figure 16. SDS-PAGE gel of all the fractions collected in the downstream processing of polyclonal IgG digestion mixture. **1** - Molecular weight ladder; **2** - Digestion Mixture; **3** - protein A flow-through; **4** - protein A elution; **5** - Protein L flow-through; **6** - protein L elution. Digestion were carried out using the following conditions: 24 hours of digestion, 0.20 mg papain/mL, 1 mg IgG/mL, 40ºC.

After the chromatographic runs, additional diafiltration steps were carried out with the aim of concentrating the different fractions collected, i.e., Fc fragments, kappa Fabs and lambda Fabs; of eliminating impurities (e.g. papain in protein L flow-through, non-digested antibody in protein A elution) and of exchanging the buffer to PBS. In the end, the concentration of each fragment was determined by reading the absorbance of each sample at 280 nm, using a calibration curve with fixed concentrations of antibody. Even though, this method has some sources of error, it was the best method found for antibody-derived fragments quantification. It assumes that each fraction has only pure Fab or Fc, which may not be completely true, since some small traces of impurities may be present. Also, the use of

undigested antibody to construct the calibration curve, in alternative to the use of fragments with well-defined concentrations, can introduce a deviation from the real concentration value.

For the high throughput screening of resins and chromatographic conditions, some methods are based on fluorescent measurements of fluorophores coupled to target molecules. However, the attachment of these fluorescent molecules can, in many cases, affect the properties of the target molecules, thus influencing the results[85]. Because of that, the IEF technique was applied to check if the coupling of BODIPY™ TMR NHS to IgG fragments was affecting their properties, allowing the determination of pI ranges from Fc and kappa and lambda Fab fragments and the comparison between labelled and non-labelled proteins (**Figure 17**). Also, kappa Fab fragments labelled with another fluorophore, BODIPY™ FL NHS ester, were analysed. In all the cases, the multiple bands observed for labelled proteins were also visible in the corresponding non-labelled samples, meaning they have similar charges. In addition, the IEF gel presented several bands in each lane, which can be explained by the fact that Gammanorm® IgG is a mixture of antibodies, and so, different isotypes and subclasses with varying isoelectric points are present in solution.

Overall, these results suggest that both fluorophores analysed can be used as a tool for downstream studies employing high throughput methods based on fluorescence, specially purification methods based or affected by charge phenomena. Nonetheless, the hydrophobicity conferred by the phenyl groups of BODIPY fluorophores must be taken into account, since they can enhance hydrophobic interactions, leading to less accurate results[85].

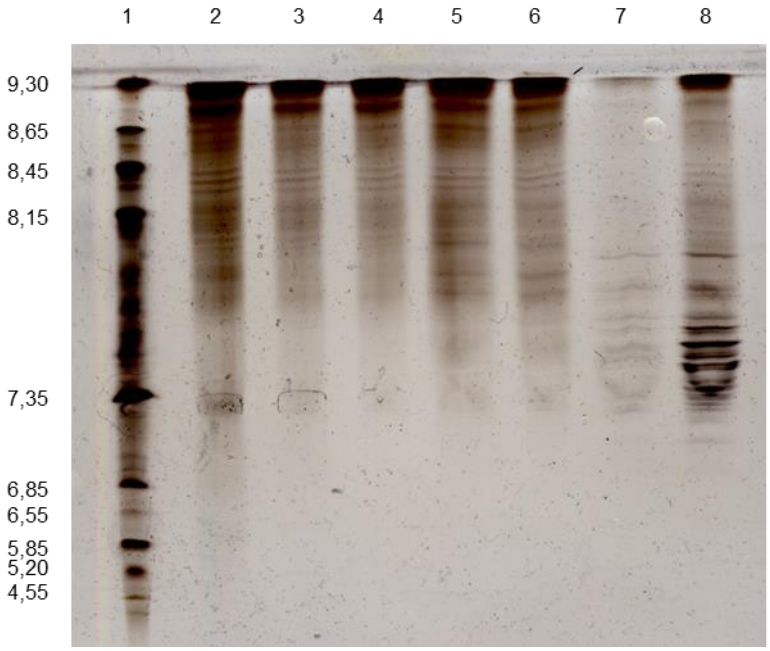

Figure 17. Isoelectric focusing gel of Gammanorm® derived fragments **1** - Marker; **2**- Labelled kappa Fabs (BDP FL NHS); **3** - Non-labelled kappa Fabs; **4** - Labelled kappa Fabs (BDP TMR NHS); **5** - Non-labelled lambda Fabs; **6** - Labelled lambda Fabs (BDP TMR NHS) ; **7** - Non-labelled Fc fragments; **8** - Labelled Fc fragments (BDP TMR NHS).

4.3. High-throughput screening of phenylboronate chromatographic conditions

4.3.1. Binding Studies

As previously discussed in the introduction chapter**,** there is currently no standard method to purify Fabs. If it is true that protein L remains the only affinity ligand able to directly bind to Fabs, its application is restricted to fragments containing kappa light chains. Alternatively, a set of non-affinity based methods can be used, but none offers the specificity and universality of protein A to purify mAbs[7,50]. Therefore, the study of substitute affinity ligands towards Fab fragments is required to develop a broader purification process, regardless its structure and manufacturing method and platform being used.

To assess the possibility of using aminophenylboronate as a multimodal ligand with affinity for cis-diol groups, present in kappa and lambda Fabs, a microfluidic platform developed by Pinto and co-workers was used, which allows the rapid screening of operational conditions with a minimum consumption of reagents and biomaterial[8]. After performing the experiments, fluorescence data was extracted and adjusted to the Hill model, allowing the determination of the F_{max} for each condition. This parameter corresponds to the maximum fluorescence intensity value when ligand is saturated. The device was firstly employed to test different adsorption conditions, including 5 different salt concentrations, ranging from 0 mM to 200 mM of NaCl, and 3 pH values, including 5, 7 and 9.2, in 50 mM acetate, phosphate and carbonate buffers, respectively. Also, 1 M of NaCl was tested to confirm that a sharp increase in salt concentration would not considerably affect adsorption, which was true for all cases. The results represented in **Figure 18.** were normalized considering the highest Fmax for each target molecule: 24.9 a.u. at pH 5 using 150 mM NaCl and 27.6 a.u. at pH 5 using 50 mM NaCl, for kappa (DOL=0.344) and lambda (DOL=0.301) respectively. Looking at the presented heatmaps, binding

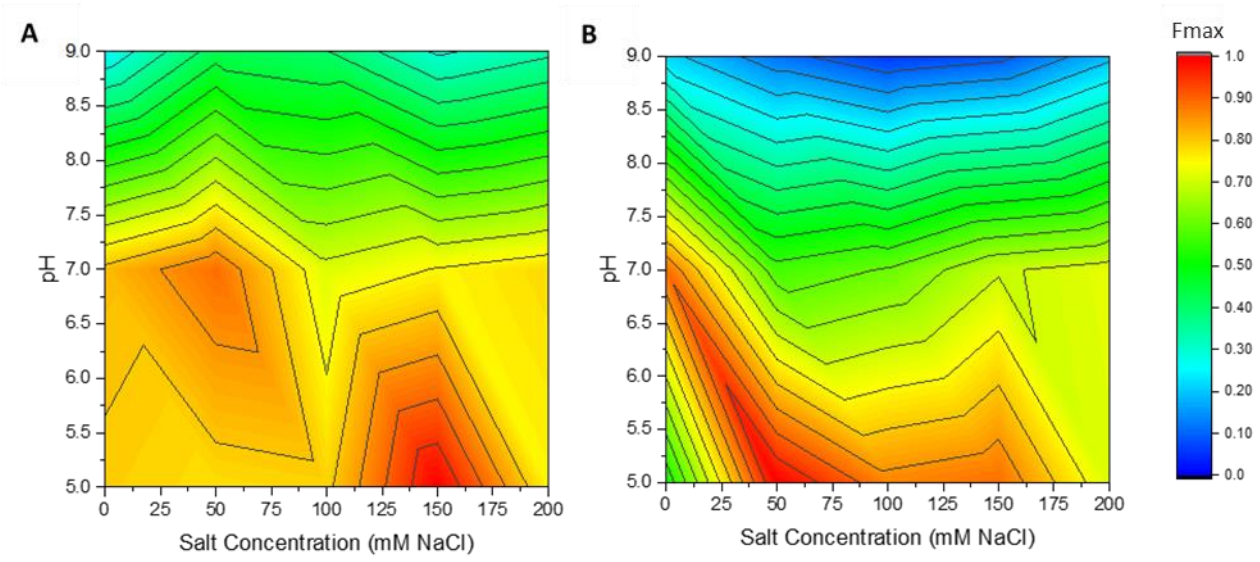

Figure 18. Relative adsorption of kappa (**A**) and lambda (**B**) Fab fragments to aminophenylboronate, under different pH values (5,7 and 9.2) and salt concentrations (ranging from 0 to 200 mM NaCl). Fluorescence values were adjusted to the Hill enzymatic kinetics model, which produced a Fmax for each condition, corresponding to maximum adsorption when ligand is saturated. Results were normalized, considering the highest value. DOL kappa Fabs: 0.344; DOL lambda Fabs: 0.301.

of kappa and lambda Fabs to aminophenylboronate was enhanced at pH 5, under intermediate ionic strength, and at pH 7, using no salt or lower salt concentrations. In contrast, at pH 9.2 and for all salt concentrations tested, Fmax values are lower, which means a less significant binding is taking place under these conditions. In fact, when environmental pH is higher than boronic acid pKa, around 8.8-8.9, aminophenylboronate adopts a tetrahedral conformation, which is negatively charged[58]. Because the pI of most of Fabs is lower than 9.2, as it was previously observed in **Figure 17**, negatively charged fragments are predominant, resulting in electrostatic repulsion between ligand and target molecules. This phenomenon is probable leading to suppression of specific binding, since Fabs are not able to make the necessary surface contact with the ligand. Interestingly, an increase in ionic strength should have been enough to supress electrostatic interactions and enhance affinity binding, but this was not observed, even when using 1 M NaCl[62].

Regarding the results at pH 5 and 7, aminophenylboronate is expected to be predominantly in a neutral trigonal conformation, which has lower affinity towards molecules containing cis-diol groups. Yet, in this conformation, the ligand has an empty orbital in the boron atom, becoming a Lewis acid ready to accept a pair of electrons from a Lewis base. Potential electrons donors include unprotonated amines or carboxyl groups present in several amino acids or even components of the adsorption buffers, such as phosphate (PO_4^{-3}), acetate ($C_2H_3O_2^-$) or the chloride ion (Cl^-) from NaCl. Either way, when this coordination reaction happens, ligand conformation is switched to tetrahedral, promoting in some cases higher affinity interactions and PB specificity[72,73]. Thus, since these Lewis bases are present in all the conditions tested, this secondary interaction is probably taking place, enhancing primary interaction of Fabs to aminophenylboronate. Moreover, at these pH values, fragments tend to be positively charged, since none of them present an isoelectric point below 7.35 (see **Figure 17**). This means electrostatic attraction between negative ligand and positive Fabs can be occurring, increasing protein retention. None the less, even if this is happening, electrostatic interactions seem not to be the driving force of the chromatography process, since the use of higher salt concentrations did not have a significant impact on the results. Other possibility is that hydrophobic interactions, which are enhanced under a higher ionic strength, can be balancing the suppression of the electrostatic interactions.

Then, for the same operating conditions, other target molecules were further assessed, including impurities from of enzymatic cleavage of antibody, namely both full-sized antibodies (DOL=2.75) and Fc fragments (DOL=0.277), and from recombinant production using mammalian cells namely molecules present in a CHO-S supernatant, including undesirable proteins, lipids and nucleic acids produced by the host cells. The results obtained are shown in **Figure 19**. In all the cases, binding to aminophenylboronate was less significant at pH 9.2, probably because of the electrostatic repulsion discussed above. In fact, the isoelectric points of most of Fc fragments (see **Figure 17**), full-size antibodies and proteins from CHO-S supernatant (see **Figure A1** in appendix) are located below 9.2, meaning they have a predominant negative charge under these conditions. Moreover, while undigested antibody (maximum value of Fmax = 23.9 u.a.) and CHO-S supernatant adsorption (maximum value of Fmax = 76.8 u.a.) did not significantly changed with ionic strength, binding of Fc to aminophenylboronate was maximized using 200 mM NaCl at pH 7 and no added salt at pH 5, presenting Fmax of 13.6 and

11.9 u.a., respectively. This can suggest the presence of hydrophobic and electrostatic interactions, which are enhanced in the presence of higher and lower ionic strengths, respectively[62]. Since, below ligand pKa, adsorption of Fab and Fc fragments is salt-dependent, on contrary to what was observed for the whole antibody, ionic and hydrophobic interactions are probably having a more relevant role in first case. In fragments, the digestion of the antibody can result in the exposure of hydrophobic and charged amino acids, being those proteins more prone to the establishment of hydrophobic/electrostatic interactions.

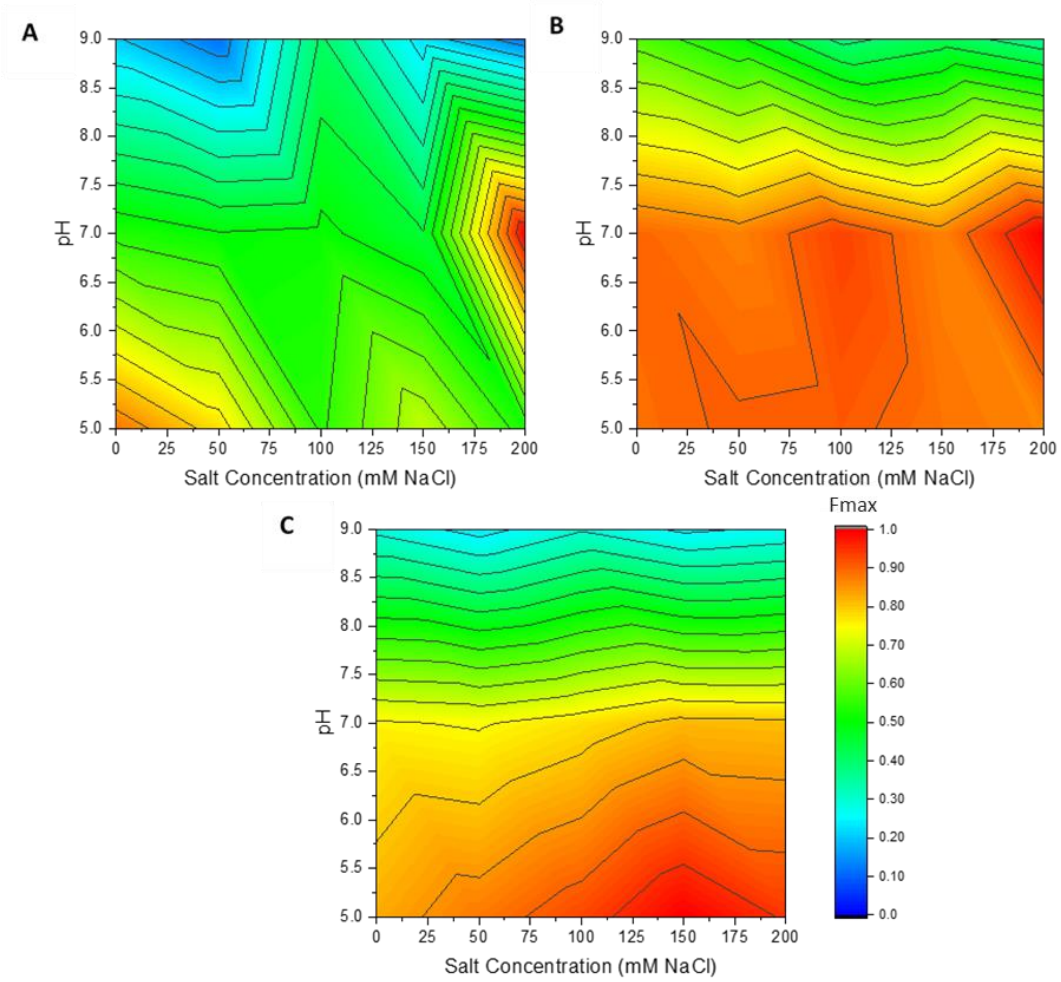

Figure 19. Relative adsorption of Fc fragments (**A**), undigested polyclonal antibody mixture (**B**) and proteins from CHO-S supernatant (**C**) to aminophenylboronate, under different pH values (5,7 and 9.2) and salt concentrations (ranging from 0 to 200 mM NaCl). Fluorescence values were adjusted to Hill model, which produced a Fmax for each condition, corresponding to maximum adsorption when ligand is saturated. Results were normalized, considering the highest value. DOL FC fragments = 0.277; DOL Gammanorm® = 2.75

For both Fab isotypes and Fc fragments, alternative buffers to carbonate and phosphate were tested, including EPPS pH 7 and CHES pH 9.2 buffers, respectively. Their chemical structure is similar to HEPES, which presents tertiary amines, responsible for donating electrons to boron atom during coordination interaction[72]. As mentioned before, increased affinity of target molecules to aminophenylboronate is associated with this electron transfer reaction. Two different salt concentrations

were tested, including 0 mM and 150 mM NaCl. Results are represented in **Table 2**. Overall, the Fmax values obtained indicate lower or similar biding to the column, except for kappa and Fc at pH 9.2 no NaCl added, probably because charge transfer interactions were already taken place. Because EPPS and CHES did not produced better results and they present significantly higher purchase prices, phosphate and carbonate were maintained as adsorption buffers.

Table 2. Fmax values in arbitrary units obtained for adsorption of Kappa and Lambda Fabs and Fc fragments to aminophenylboronate, using different binding buffers: Phosphate and EPPS at pH 7 and Carbonate and CHES at pH 9.2

		Phosphate pH 7	EPPS pH 7	Carbonate pH 9.2	CHES pH 9.2
Kappa	0 mM NaCl	20.2	19.4	6.4	21.4
	150 mM NaCl	18.8	11.0	7.3	5.2
Lambda	0 mM NaCl	24.6	14.7	6.0	5.0
	150 mM NaCl	19.1	13.8	2.4	2.1
Fc	0 mM NaCl	7.2	5.4	2.8	10.5
	150 mM NaCl	6.1	7.8	3.0	0.6

Finally, to compare the results obtained using phenylboronate to protein L, the same method was used to assess kappa Fabs adsorption to this affinity ligand. Since the amount of sample and the biological material introduced in the microfluidic column were the same, results could be directly compared, which was not possible for different biological materials with different degrees of labelling. As it can be observed in **Figure 20**, maximized adsorption to protein L is achieved at pH 5 for 50 mM NaCl, corresponding to a Fmax of 25.1. On the other hand, optimized binding to phenylboronate is

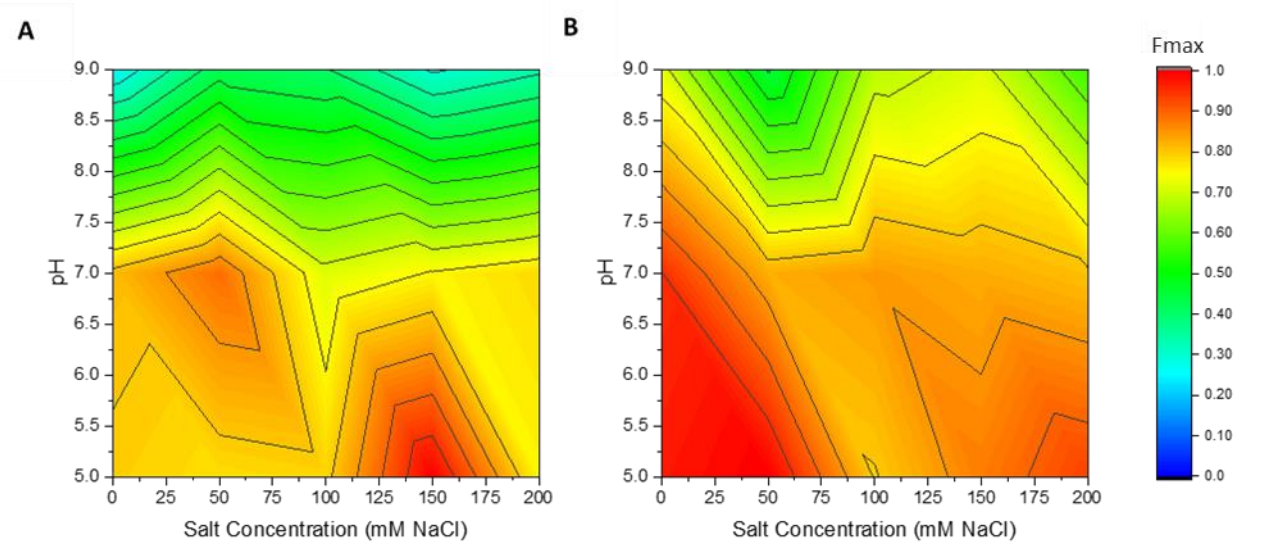

Figure 20. Relative adsorption of kappa Fabs to aminophenylboronate (**A**) versus to protein L (**B**), under different pH values (5,7 and 9.2) and salt concentrations (ranging from 0 to 200 mM NaCl). Fluorescence values were adjusted to the Hill enzymatic kinetics model, which produced a Fmax for each condition, corresponding to maximum adsorption when ligand is saturated. Results were normalized, considering the highest value.

observed at pH 5 and 150 mM NaCl, corresponding to a Fmax value of 24.9. These results suggest that both ligands could be used as a tool to purify kappa Fabs with similar efficiencies. Also, given that affinity ligands, as protein L, are generally much more expensive, phenylboronate could be used as a cheaper alternative, but further studies should be performed to explore this possibility.

4.3.2. Elution Studies

The next step was to screen different elution conditions of Fabs from aminophenylboronate at microscale. The method used was adapted by adding an additional step, which consisted in flowing the elution buffer into the microchannel under a fluorescence microscope. This allowed the monitoring of fluorescence decay as Fabs were being eluted from the column. A total of six different elution agents were tested, including Tris, D-sorbitol and magnesium chloride at concentrations ranging from 0 to 2 M and guanidine hydrochloride, urea and arginine at lower concentrations from 0 to 1 M. Also, for all of them the pH was maintained at 8.5, by adding 150 mM Tris-HCl. Adsorption was performed using 50 mM phosphate buffer at pH 7, with no salt added, which was also used as a negative control during elution. Results for all the conditions tested can be observed in **Figure 21**. Slope of the decrease of fluorescence intensity with time for each condition were calculated for the first 15 seconds, which are presented in **Table A1** to **Table A6** in the appendix section.

Looking at the results, elution of Fabs from aminophenylboronate was more efficient using Tris as elution buffer. For this agent, the best conditions were 0.5 M Tris-HCl for kappa (-3.36 %/s) and 1.75 M Tris-HCl for lambda Fabs (-4.32 %/s). In fact, Tris has been used to remove full-size monoclonal antibodies from phenylboronate, due to its capacity to disrupt not only affinity bonding, but also secondary interactions, working as a competitor for the ligand via esterification and coordination interaction[6]. The best results obtained with Tris were followed by guanidine hydrochloride and arginine, also effective in eluting Fabs, being the best conditions 1.0 M guanidine hydrochloride (-2.96 %/s) and 0.5 M arginine (-2.87 %/s) in the case of kappa, and 0.5 M arginine (-4.01 %/s) and 1.0 M guanidine hydrochloride (-3.70 %/s), in the case of lambda Fabs. Besides supressing aggregation and promoting protein renaturation, arginine has been used as elution agent for monoclonal antibodies in several types of chromatography, including protein A affinity chromatography and multimodal cation exchange chromatography (e.g. Capto MMC, which is based on hydrophobic and electrostatic interactions). It affects all the secondary interactions present in aminophenylboronate multimodal chromatography, such as hydrophobic and electrostatic interactions and hydrogen bonding, as well as affinity interactions, because of its tendency to accumulate in protein surfaces, specifically near aromatic, polar and charged aminoacids, reducing interaction with the column[86,87]. On the other hand, guanidine, as well as urea, are denaturing and chaotropic agents, responsible for disruption of hydrophobic interactions and other non-electrostatic interactions[86]. In the case of denaturing agents, change in tertiary structure can lead to loss of affinity to the ligand. Therefore, the most efficient agents were the ones interfering with both affinity and non-affinity binding. Producing worst elution results were D-sorbitol (maximum slopes of -2.01 %/s and -3.00 %/s, for 1.0 M and 1.5 M sorbitol and kappa and lambda Fabs, respectively), a competitor to specific interactions with high affinity towards APB[64], magnesium chloride (maximum slopes of -2.62 %/s

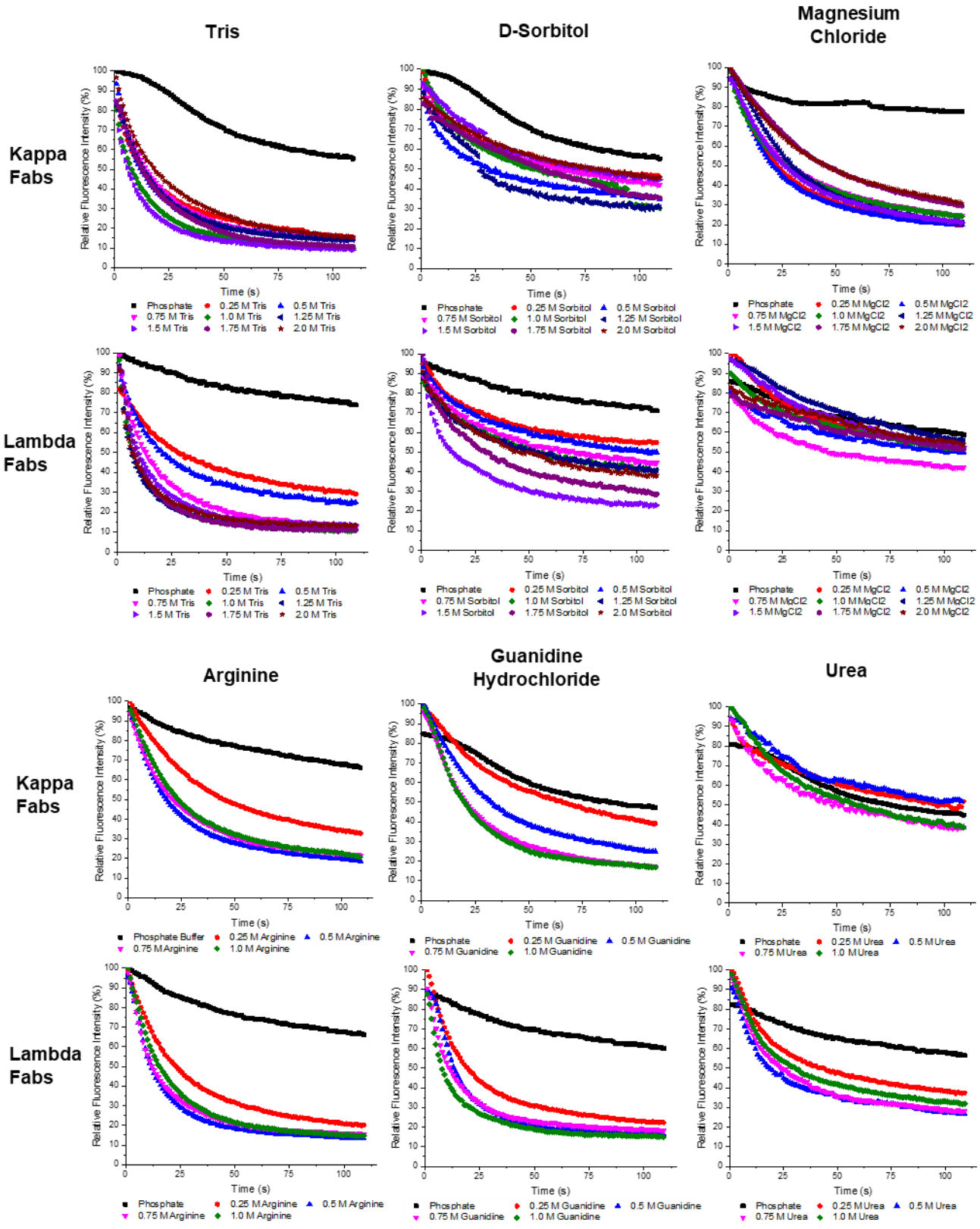

Figure 21. Decay of relative fluorescence over time, corresponding to elution of kappa and lambda Fabs from aminophenylboronate, using different elution buffers: Tris, Sorbitol, Magnesium chloride, Arginine, Guanidine hydrochloride and Urea. All of them contain 150 mM Tris-HCl as buffer to maintain a pH of 8.5. Adsorption is performed using 50 mM phosphate as binding buffer.

and -1.31 %/s, for 0.25 M $MgCl_2$ and kappa and lambda Fabs, respectively), a chaotropic salt which affects electrostatic interactions and possibly π-π complexation but has been reported as an enhancer of cis-diol affinity interactions[5], and urea (maximum slopes of -1.67 %/s and 2.75 %/s, for 0.75 M and 0.5 M urea and kappa and lambda Fabs, respectively). Overall, results show that agents with the ability of interfering with both cis-diol affinity bonding, but also with non-covalent bonding, especially hydrophobic and electrostatic interactions, generate maximized elution of Fabs from aminophenylboronate. On the other hand, D-sorbitol and magnesium, chloride, that only negatively affect primary or secondary interactions, respectively, are among the worst elution agents tested. This suggests that a synergetic effect between covalent affinity binding and secondary interactions is leading to target molecule adsorption.

Another relevant aspect is that, generally, maximum slopes were obtained for intermediate concentrations of elution agents, all equal to 1.0 M or lower, except for lambda Fabs when using Tris and D-sorbitol, which required the use of 1.75 and 1.5 M of elution agent, respectively, for maximized elution. This is clearly visible in the graphs, as results tend to become homogenous generally for concentrations higher than 0.5 M of elution buffer. In the case of magnesium chloride, the best results were achieved when using only 0.25 M $MgCl_2$, which can be explained by the fact that affinity binding is being enhanced, even though non-specific interactions are being supressed. The use of lower concentrations of the elution agent allows saving reagents, especially important for chromatographic processes using expensive reagents as arginine. In this case, maximum recover of target molecules was achieved using 0.5 M arginine for both classes of Fabs, half of the highest concentration tested.

Also important is the fact that, sometimes, divergent results were obtained for kappa and lambda Fabs. For example, while magnesium chloride could be used to elute the kappa isotypes, as a maximum slope of -2.62 %/s was achieved when using 0.25 M $MgCl_2$, in the second case slopes are not far from the negative control. The opposite situation was observed for urea. Moreover, the highest slope values were obtained for lambda isotypes, except in the case of magnesium chloride. This may indicate that different types of interactions are having varying relevance in the adsorption process of each class of fragments to aminphenylboronate and so, light chain plays an importance role in the process. The availability of different interacting groups may also be different in different isotypes of Fabs.

Concluding, the microfluidic approach used was useful to test a large set of operational conditions and target molecules in a relatively short period of time and in a cost-effective manner. However, in the case of adsorption, it does not allow direct comparison of the results between different target molecules, because they present a different number of fluorophores attached to their molecular structure, which can also be affecting the results. Moreover, it does not give any information about the proportion of molecules attached to the beads versus the molecules in the flow-through. So, studies at the macroscale are required to extract this information, but also for validation of the results at microscale.

4.4. Validation of the microfluidic results at macroscale

4.4.1. Adsorption studies

The next step was to validate the previous results at macroscale, using an ÄKTA™ Purifier 10 System, which allows protein detection by reading its absorbance at 280 nm. For this, a total of five conditions were chosen as representative of the data set produced at microscale: 50 mM phosphate buffer pH 7 for three different salt concentrations, including 0, 50 and 150 mM NaCl, 50 mM acetate buffer 150 mM NaCl pH 5 and 50 mM carbonate buffer 150 mM NaCl pH 9.2. 1 M Tris-HCl was chosen as the standard elution buffer, as it produced good results for Fabs elution. These conditions were tested for adsorption of both Fabs isotypes, as well as impurities from distinct fragments manufacturing method: Fc fragments (digestion) and CHO-S supernatant (recombinant production). A negative control consisted in the injection of adsorption buffer, whose chromatogram was subtracted to every chromatogram obtained. Chromatograms for all the target molecules tested are shown in **Figure 22**. Also, considering the peak area corresponding to flow-through and elution, a ratio between elution and total area was calculated for each condition. Results are shown in **Table 3**. In addition, a single injection of Gammanorm® IgG was performed at pH 7 with no salt added, which resulted in the recovery of 99.24% of proteins in the elution fraction. Finally, SDS-PAGE analysis for different fractions corresponding to kappa and lambda Fabs FT and elution E was performed with silver staining for better visualization of the protein bands. Gels can be observed in **Figure 23** and **24**.

The results obtained at macroscale follow the conclusions of the studies at microscale. Firstly, at pH 9.2, adsorption of fragments is less significant than at pH 5 and 7, as the FT fraction shows higher peak area and the E fraction is almost inexistent. As mentioned before, under these conditions low binding occurs probably due to electrostatic repulsion, which does not allow the protein to make the surface contact needed for the establishment of the covalent bonds. In opposition, binding at pH 5 and 7 is much higher for antibody-derived fragments, as a maximum increase of 14.68, 26.73 and 73.38 % in ratios of E/total peak areas were observed for kappa and lambda Fabs and Fc fragments, respectively, when comparing with results obtained at pH 9.2. Under these conditions, coordination interaction is probably responsible for switching the ligand from the trigonal to the tetrahedral conformation, promoting the affinity covalent interactions. Moreover, electrostatic attraction between positive target molecules and negative ligand can be involved. In the case of proteins from CHO-S supernatant, results were approximately the same at pH 5, 7 and 9.2, because these impurities have almost no binding for all tested conditions. In the microfluidic studies, these components were observed to have a significantly higher binding at pH 5 and 7 than at pH 9.2, but this did not happen here, probably because other labelled components of the supernatant, not read at 280 nm, are interfering with the results at microscale. For all target molecules, the ratio between elution and total area was similar for different NaCl concentrations at pH 5 and 7, except for kappa Fabs and Fc fragments, which demonstrate lower binding when using acetate and phosphate 150 mM NaCl, respectively, as binding buffer. These results suggest the importance of electrostatic interactions in those cases, as a suppression of these interactions is observed when ionic strength is increased.

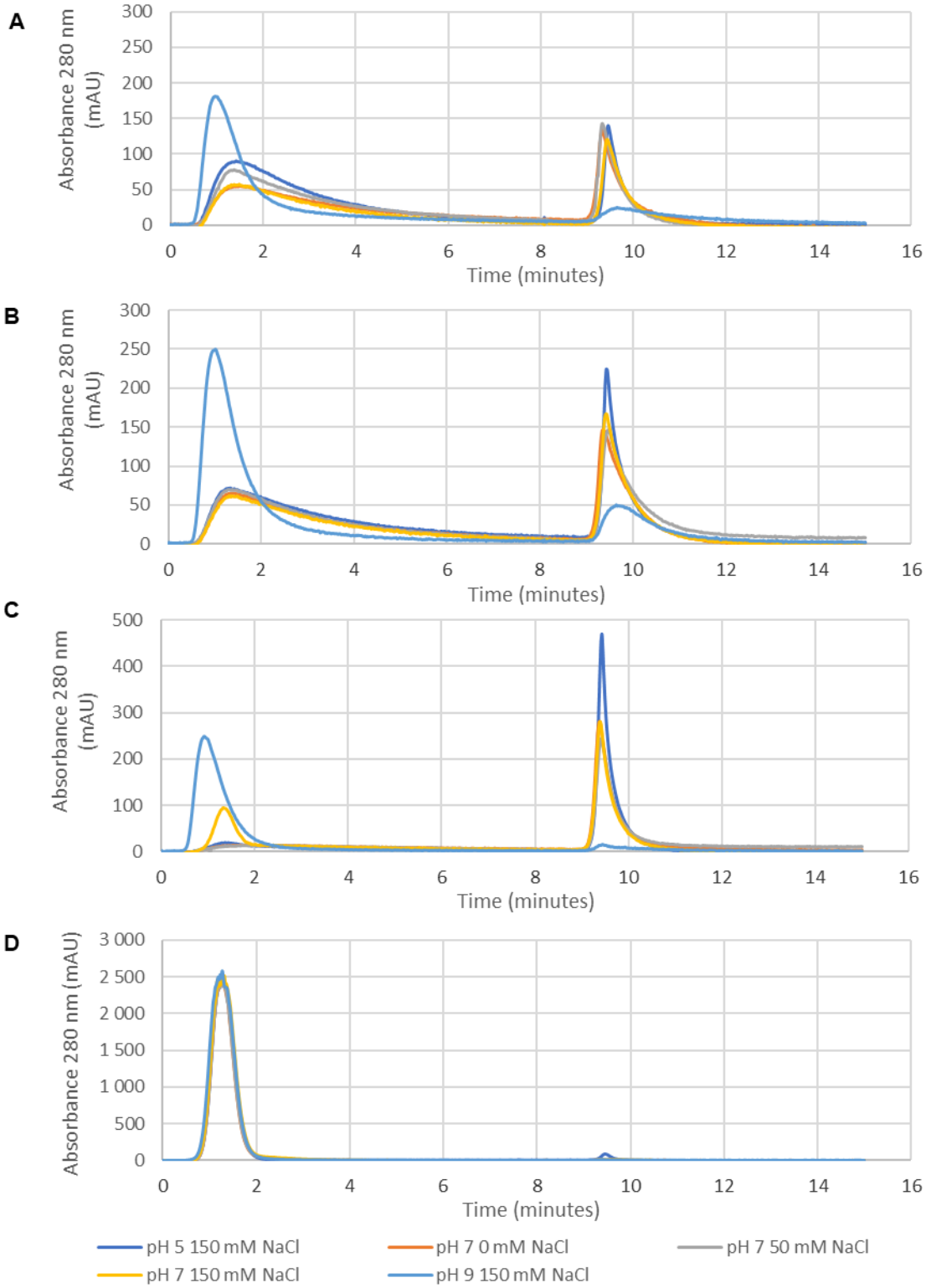

Figure 22. Adorption Studies of different target molecules to phenylboronate: **A.** Kappa Fabs; **B.** Lambda Fabs; **C.** Fc Fragments; **D.** CHO-S supernatant. 50 mM acetate 150 mM NaCl, 50 mM Phosphate 0, 50 and 150 mM NaCl and 50 mM carbonate 150 mM NaCl were used as adsorption buffers. **0-8 min**: Adsorption; **8-15 min**: Step Elution 1 M Tris pH 8.5.

Table 3. Ratio between elution and total peak areas, for kappa and lambda Fabs, Fc fragments and CHO-S supernantant, using different adsorption buffers (acetate, phosphate and carbonate) and salt concentrations (0, 50 and 150 mM NaC).

	Kappa Fabs	Lambda Fabs	FC Fragments	CHO-S Supernatant
Acetate buffer pH 5 150 mM NaCl	27.9%	42.6%	82.7%	2.0%
Phosphate buffer pH 7 no salt	34.2%	45.6%	85.4%	2.1%
Phosphate buffer pH 7 50 mM NaCl	34.4%	48.4%	80.2%	0.7%
Phosphate buffer pH 7 150 mM NaCl	34.8%	46.6%	73.2%	1.0%
Carbonate buffer pH 9 150 mM NaCl	20.1%	21.6%	12.0%	1.0%

Apart from the validation of the previous results, experiments at macroscale also allowed comparative results between different biomaterials and the measurement of protein that binds to the column versus the protein in the FT, not possible at microscale. For example, CHO-S supernatant was almost completely recovered in the FT fraction, proving its inability to bind to aminophenylboronate under all the tested conditions, even though it showed the highest fluorescence values in the screening step. This was probably due to the fact that not only proteins were labelled with the fluorophore for the microfluidic experiments, but also other molecules present in the cell culture supernatant (lipids, nucleic acids and other compounds), that are not detected at 280 nm. In opposition, Gammanorm® IgG had almost 100% of recovery in the E fraction, while the fragments showed a different binding to the ligand. Fc fragments had a maximum recovery of 85.40%, while lambda and kappa Fabs had a value of 48.35% and 34.80%, respectively. The results obtained suggest one of two things: Fc and Fab regions have a combined effect on binding of the whole antibody to APB or the hinge region, where papain cut the IgG molecule, is important in the adsorption process of full-sized antibodies. In addition, enzymatic cleavage can be affecting tertiary structure, decreasing fragments retention in the column, when compared with the respective antibody.

Moreover, looking at SDS-PAGE gels, it can be observed that bands around 50 kDa, corresponding to Fabs, and other bands around 25 kDa, corresponding to smaller fragments, such as free light chains, are present in both the FT and E fractions. Since the experiments were carried out using fragments obtained from the enzymatic cleavage of polyclonal antibodies, it is possible that differential separations are occurring according to the IgG isotype. To prove this, further tests would be needed. If this is true, aminophenylboronate could be used as a tool to purify certain isotypes of Fabs, but not as a universal tool as it is observed for Gammanorm®. Also, it would only be useful in two situations: for the downstream processing of fragments produced in recombinant systems, in the case where fragments totally bind to the column and proteins present in CHO-S supernatant are washed out, or for fragments produced by enzymatic cleavage if Fab fragments show no affinity towards the ligand and the remain impurities adsorbed to aminophenylbooronate.

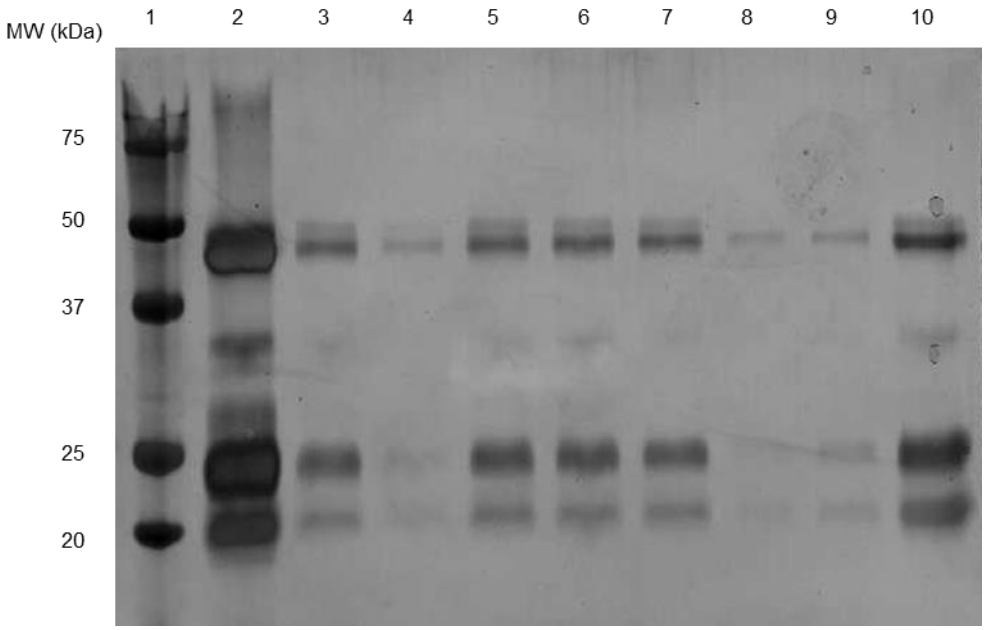

Figure 23. Silver stained SDS-PAGE gel for different fractions of aminophenylboronate chromatography, using kappa Fabs as target molecules. 50 mM Phosphate pH 7 and 1 M Tris-HCl pH 8.5 were used as adsorption and elution buffers, respectively. **1** - Protein Marker; **2** - Injection Sample; **3** - Pool of FT fractions; **4** to **6** - FT fractions; **7** - Pool of E fractions; **8** to **10** - E fractions

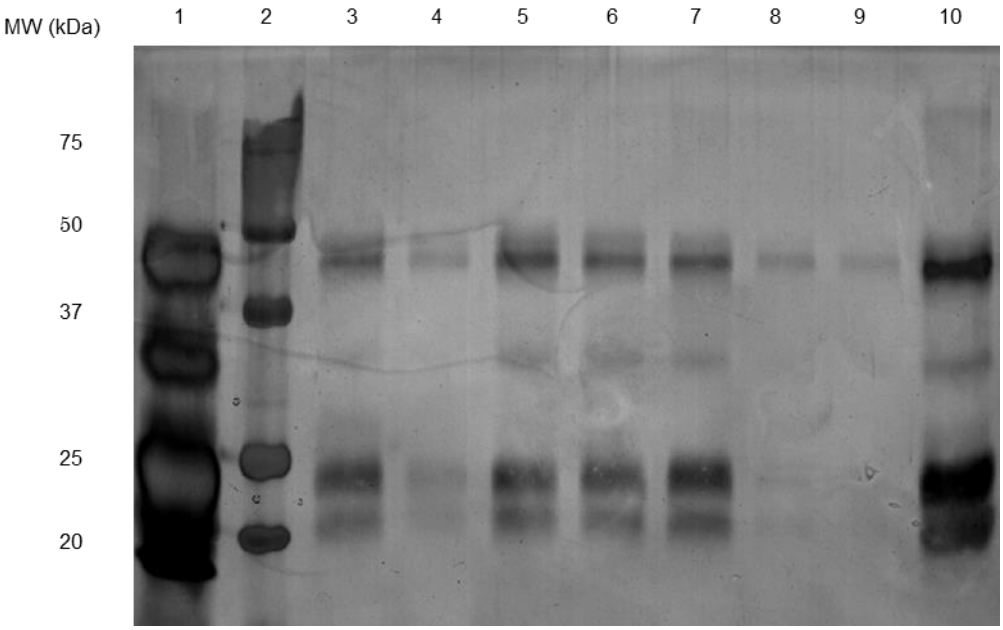

Figure 24. Silver stained SDS-PAGE gel for different fractions of aminophenylboronate chromatography, using lambda Fabs as target molecules. 50 mM Phosphate pH 7 and 1 M Tris-HCl pH 8.5 were used as adsorption and elution buffers, respectively. **1** - Injection Sample; **2** - Protein Marker; **3** - Pool of FT fractions; **4** to **6** - FT fractions; **7** - Pool of E fractions; **8** to **10** - E fractions.

4.4.2. Elution studies

A validation of the elution results obtained with the microfluidic chromatographic device was also performed at macroscale, using the same procedure described for the adsorption studies. For this, Tris and arginine were chosen once they produced the best results, along with D-sorbitol, which was the only elution agent used that interferes solely with cis-diol affinity interactions. A concentration of 150 mM Tris-HCl pH 8.5 was tested as a control. Although guanidine hydrochloride produced good results in the microfluidic studies, it was excluded because of its protein denaturating activity. For the three elution agents, a linear gradient elution (**Figure 25**) and a step gradient elution of Fabs at three different buffer concentrations, including 20, 35 and 50% of elution buffer (**Figure 26** and **27)**, were performed. Here, apart from the confirmation of the results for kappa and lambda Fabs, also Fc fragments and Gammanorm® IgG elution were studied, to check the possibility of differential retention in the column. A negative control consisting of adsorption buffer was carried out and subtracted to each chromatogram obtained. After the chromatographic runs, the efficiency of each buffer was assessed by calculating the ratios of elution peak to total area (**Table 4**). In the case of whole antibody, since it did not present a FT peak, results are shown as elution peak areas.

Looking at results (**Figure 25**), elution of the different biomolecules started at minute 7, just 2 minutes after beginning of the gradient elution step. If we consider a lag between 1 and 1.5 minute, which corresponds to the time required for the buffer to reach the column, it can be concluded that target molecules start to elute almost immediately. While Tris-HCl and D-sorbitol elution took around 2 minutes and occurred before reaching 50% of elution buffer, in the case of arginine, proteins are washed out from the column for a longer period and the corresponding peak has a lower peak height. Also, Tris and sorbitol led to the acquisition of the best results, followed by arginine. Using Tris as an elution agent, Gammanorm® IgG was entirely collected in the E fraction, with maximum peak height of around 480 mAU followed by Fc fragments, where around two thirds of the molecules were collected in the E fraction, showing peak heights of approximately 180 mAU. Fab fragments presented a lower recovery, with ratios E to total peak areas of about 30 and 40%, and peaks heights of 60 and 100 mAU, for kappa and lambda Fabs respectively. For D-sorbitol, a second smaller peak is observed when stripping the column with 1 M Tris-HCl, meaning the competing agent is not able to elute all the proteins attached to the column. A control elution, using 150 mM Tris-HCl, which is present in every elution buffer, resulted in the elution of only a small fraction of the proteins and so, its addition to D-sorbitol and arginine buffers is not having a key role in the elution process.

In the step gradient elution runs (**Figures 26** and **27**), the higher the concentration of elution buffer, the closer the results would get from those obtained in the linear gradient runs and, for 50% of buffer, the results obtained in the two elution gradients were approximately the same. Here, the presence of a second elution peak is clear, when flowing 1 M Tris-HCl into the column, for all tested step concentrations of Tris, in the case of kappa Fabs, and for all the step concentrations tested of D-sorbitol and for lower concentrations of Tris and arginine in the case of lambda Fabs.

In contrast to what was concluded from the results at microscale, affinity cis-diol interactions seem to be the driving force for retention of antibodies and fragments in the column, since sorbitol,

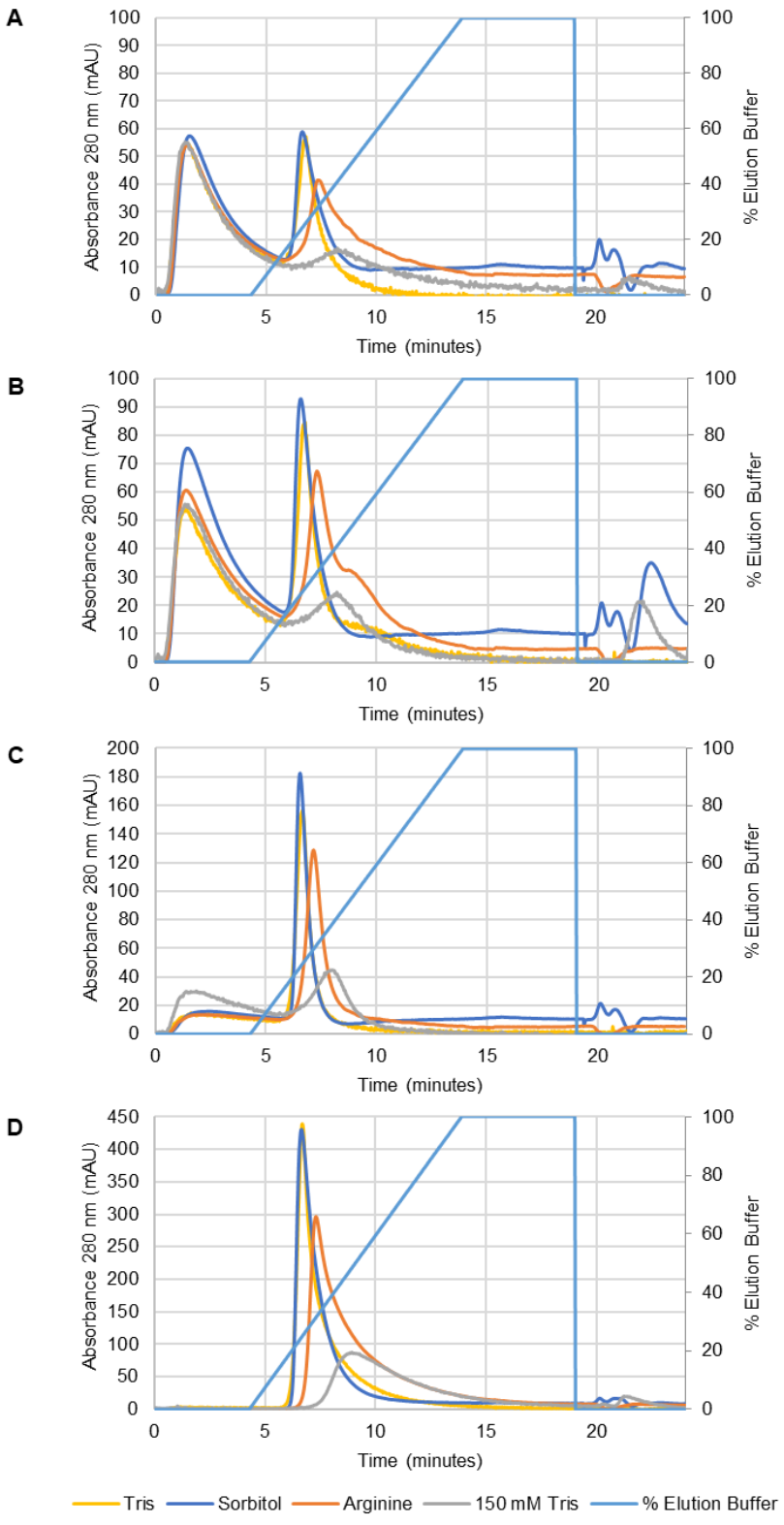

Figure 25. Testing of different buffers for elution of different target molecules from aminophenylboronate: **A**: Kappa Fabs; **B**: Lambda Fabs; **C**: Fc Fragments; **D**: Gammanorm®. **0-4 min**: 50 mM Phosphate Buffer pH 7; **4-14 min**: Gradient Elution with Tris (1 M Tris-HCl pH 8.5); sorbitol (150 mM Tris, 1 M Sorbitol pH 8.5); Arginine (150 mM Tris, 1 M Arginine pH 8.5) or control (150 mM Tris pH 8.5); **14-19 min**: Step Elution with 100% of the previous Elution Buffer; **19-24 min**: 1 M Tris-HCl pH 8.5.

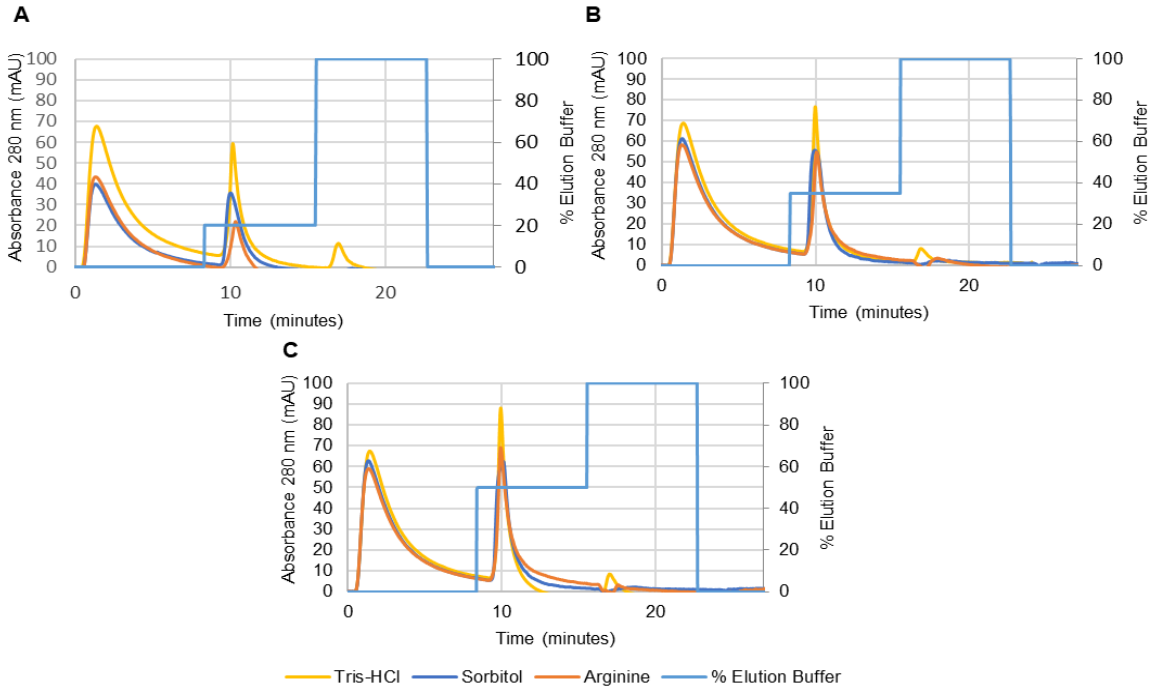

Figure 26. *Elution of Kappa Fabs from aminophenylboronate, using different concentrations of elution buffer: **A**:20%; **B**: 35%; **C**:50%. **0-8 min**: 50 mM Phosphate Buffer no salt; **8-15 min**: varying concentrations of several elution buffers, including 1 M Tris-HCl pH 8.5, 150 mM Tris 1 M Sorbitol pH 8.5; 150 mM Tris 1 M Arginine pH 8.5; **15-22 min**: 1 M Tris-HCl pH 8.5.*

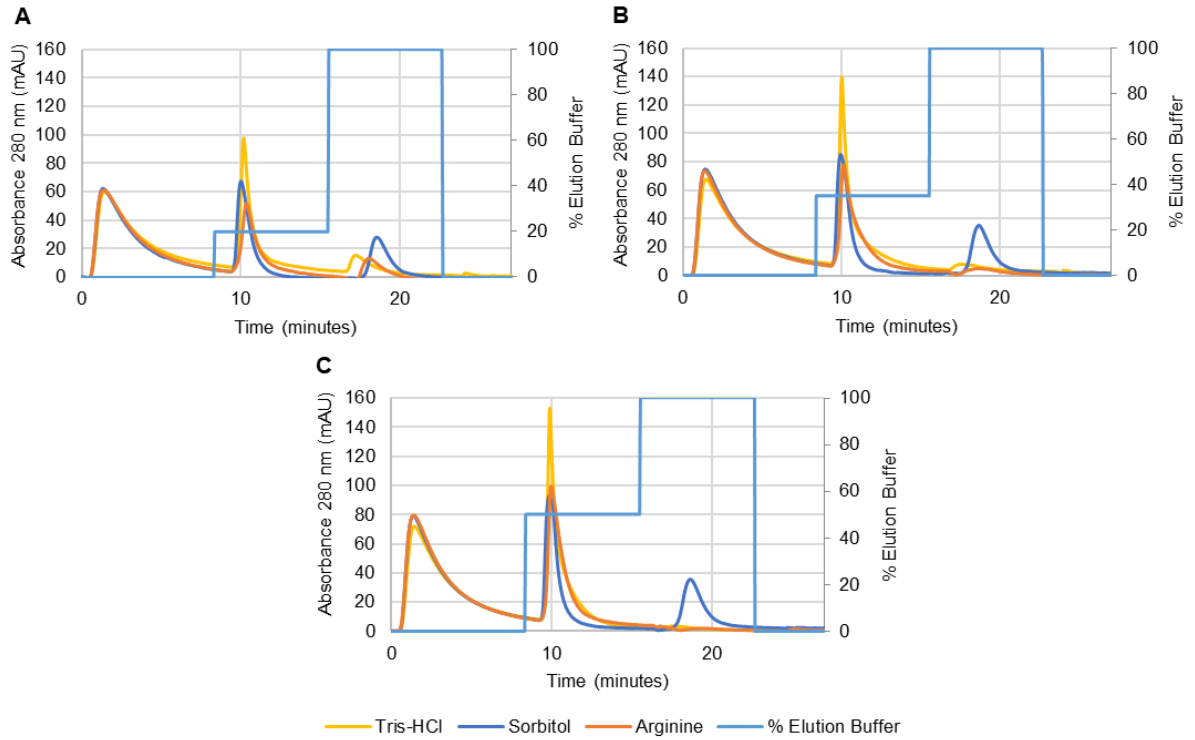

Figure 27. Elution of Lambda Fabs from aminophenylboronate, using different concentrations of elution buffer: **A**: 20%; **B**: 35%; **C**:50%. **0-8 min**: 50 mM Phosphate Buffer no salt; **8-15 min**: varying concentrations of several elution buffers, including 1 M Tris-HCl pH 8.5, 150 mM Tris 1 M Sorbitol pH 8.5; 150 mM Tris 1 M Arginine pH 8.5; **15-22 min**: 1 M Tris-HCl pH 8.5.

affecting only cis-diol primary binding, and Tris, affecting both affinity and non-affinity interactions, showed similar results. For the same reason, it can be concluded that secondary interactions do not having an important role in the process, except for lambda Fabs, as a second elution peak is observed when stripping the column with 1 M Tris-HCl, after testing sorbitol buffer. In the remaining cases, given the small impact of these types of chemical bonding (e.g. electrostatic and hydrophobic interactions) on protein retention, the presence of 150 mM Tris-HCl in the sorbitol buffer may be enough to supress them. Also, since elution of all target molecules occurred at the same time, separation of Fabs from the Fc fragments and Gammanorm® IgG by differential elution is not possible.

Overall, the microfluidic device used to screen chromatographic conditions was useful and predicted best binding and elution conditions for each target molecule. However, when using D-sorbitol as the elution agent, results at macroscale did not reflected the patterns observed at microscale, where Tris produced the best results, followed by arginine. This may be caused by the utilization of different chromatographic conditions, particularly different superficial velocities, as buffers enters the microcolumn (210 nL) at 15 µL/min, while in the ÄKTA™ Purifier 10 System, buffers flow into the 1 mL column at 1 mL/min. Because of this, in the first case, residence time of D-sorbitol is 0.28 s, too short for the agent to compete with the target molecules for the binding to aminophenylboronate, while in the case is 60 s. Thus, a higher residence time would be required to mimic with more precision conditions generally used at lab scale.

Table 4. Ratio between elution and total peaks area, for kappa and lambda Fabs and Fc fragments and elution peak area for Gammanorm®, using different elution buffers buffers: 1 M Tris-HCl pH 8.5, 150 mM Tris 1 M Sorbitol pH 8.5, 150 mM Tris 1 M Arginine pH 8.5 and 150 mM Tris-HCl pH 8.5 (control). For Fabs, beside gradient elution, also three concentrations of buffers were teste using step elution: 20, 35 and 50% of elution buffer.

	Kappa Fabs	Lambda Fabs	FC Fragments	Gammanorm®
1 M Tris-HCl pH 8.5: Gradient	33.6%	40.4%	78.5%	480 mAU/mL
Step 20%	22.2%	24.9%	-	-
Step 35%	26.7%	34.0%	-	-
Step 50%	30.6%	39.9%	-	-
1 M Sorbitol pH 8.5: Gradient	33.1%	41.1%	76.5%	484 mAU/mL
Step 20%	29.8%	27.8%	-	-
Step 35%	31.8%	32.4%	-	-
Step 50%	30.5%	35.8%	-	-
1 M Arginine pH 8.5: Gradient	24.9%	35.8%	67.8%	450 mAU/mL
Step 20%	15.4%	26.8%	-	-
Step 35%	23.6%	33.8%	-	-
Step 50%	23.0%	35.8%	-	-
150 mM Tris-HCl pH 8.5: Gradient	5.7%	3.8%	23.5%	182 mAU/mL

Finally, to check if pH was a relevant factor leading to elution of molecules from the column rather that the elution agents themselves, further experiments were performed using a pH of 7.5, below ligand pKa. Results are shown in **Table 5** and **Figure 28**.

Table 5. Ratio between elution and total peaks area, for kappa and lambda Fabs and Fc fragments and elution peak area for Gammanorm®, using different elution buffers buffers: 1 M Tris-HCl pH 7.5, 150 mM Tris 1 M Sorbitol pH 7.5, 150 mM Tris 1 M and Arginine pH 7.5.

	Kappa Fabs	Lambda Fabs	FC Fragments	Gammanorm®
1 M Tris-HCl pH 7.5: Gradient	31.0%	41.9%	57.6%	267 mAU/mL
1 M Sorbitol pH 7.5: Gradient	32.4%	39.5%	66.9%	356 mAU/mL
1 M Arginine pH 7.5: Gradient	20.8%	17.1%	23.9%	305 mAU/mL

At pH 7.5, the elution peaks obtained for all target molecules were wider, meaning it takes more time of the proteins to be washed out, and presented lower peak heights. For Fab fragments, using Tris and D-sorbitol in the elution buffer, E to total peak area ratios were similar to those obtained at pH 8.5, with the elution peak representing around 30 and 40% of the sum of all peak areas for kappa and lambda Fabs, respectively. For Fc fragments, when using these elution agents, recovery was 20 and 10% lower, respectively. On the contrary, for Gammanorm® IgG and for all target molecules when using arginine buffer, except for kappa Fabs, results were much lower than at pH 8.5, which indicates that switching the ligand conformation from the tetrahedral negative to the trigonal neutral form is relevant for elution.

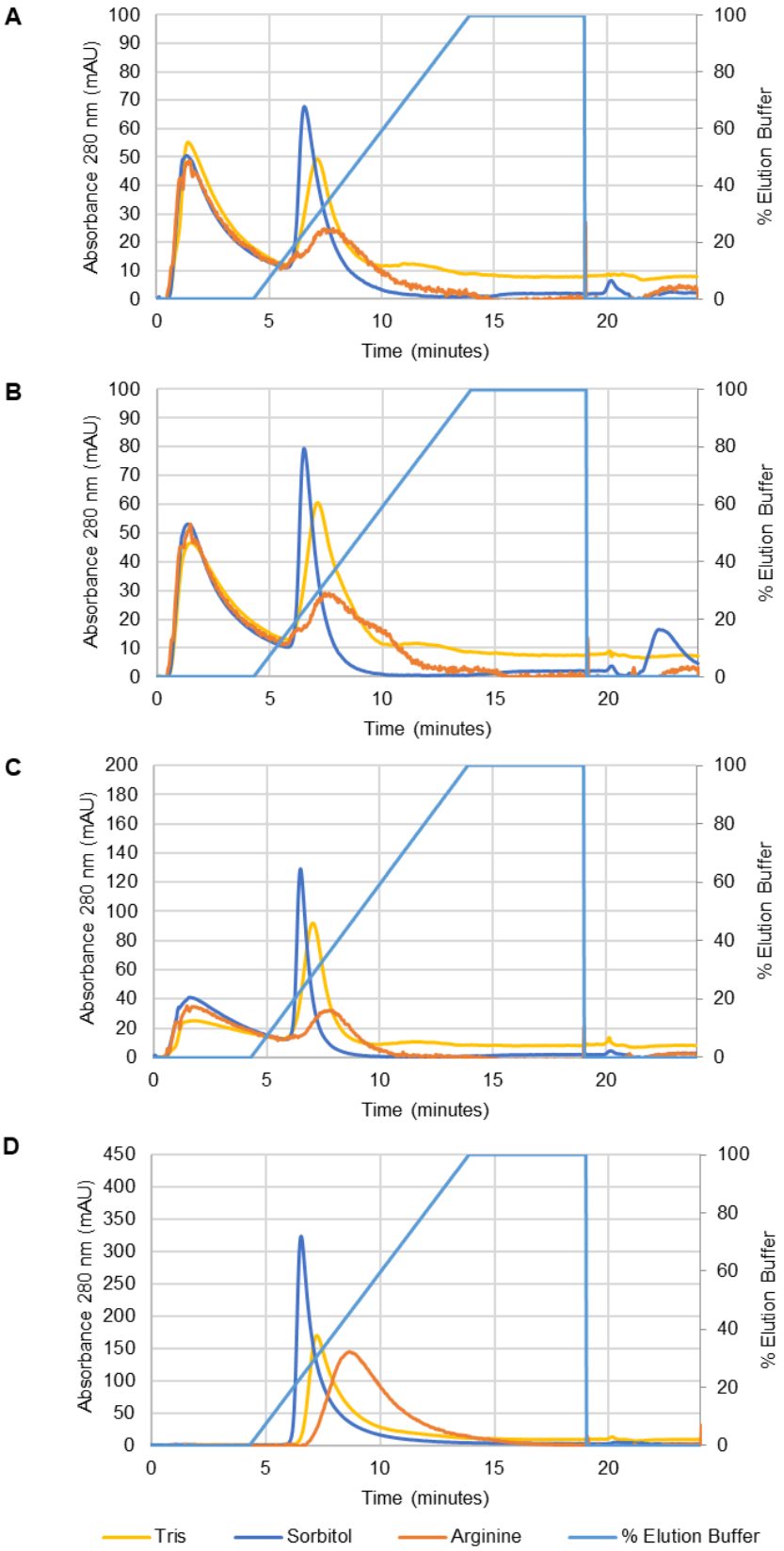

Figure 28. Testing of different buffers for elution of different target molecules from aminophenylboronate: **A**: Kappa Fabs;**B**: Lambda Fabs; **C**: Fc Fragments; **D**: Gammanorm®. **0-4 min**: 50 mM Phosphate Buffer pH 7; **4-14 min**: Gradient Elution with Tris (1 M Tris-HCl pH 7.5); sorbitol (150 mM Tris, 1 M Sorbitol pH 7.5) or Arginine (150 mM Tris, 1 M Arginine pH 7.5) **14-19 min**: Step Elution with 100% Elution Buffer; **19-24 min**: 1 M Tris-HCl pH 8.5.

5. Conclusions and Outlook

In the current work, the possibility of using aminophenylboronate as an affinity ligand in the downstream processing of antibody fragments was assessed, using a microfluidic device previous developed by Pinto and coworkers, which is based on fluorescence measurement of labelled proteins. Prior to this, screening and optimization of factors involved in the manufacturing process of Fab fragments, by enzymatic cleavage of a polyclonal mixture of antibodies, were performed. Under the optimum values of digestion time, temperature and papain and antibody concentrations, an increase of 41% in antibody digestion yield was achieved. Screening of binding conditions for kappa and lambda Fabs and impurities tested showed that binding at pH 9.2 is less significant for all of them, probably due to electrostatic repulsion between negatively charged proteins and ligand. At pH 5 and 7, proteins could bind to the column, as cis-diol affinity binding seems to be the prevalent force, enhanced by coordination reaction between a Lewis base and the ligand. Maximum binding of Fab fragments was achieved when using intermediate salt concentrations at pH 5 and lower ionic strength at pH 7. Then, elution studies at microscale showed more elution of Fabs from the column using agents affecting both specific and secondary interactions, which was the case of tris, arginine and guanidine hydrochloride. When validating these results at macroscale using an ÄKTA™ Purifier 10 System, more data could be extracted, including the ratio of protein in the elution fraction to the total of protein injected and comparison of results between different target molecules. During validation of the adsorption results, global trends observed at microscale could be confirmed. Moreover, proteins from CHO-S supernatant were almost totally recovered in the FT fraction, while the opposite situation happened for undigested Gammanorm® IgG. Fc and Fab fragments where present in both FT and E fractions. Finally, when validating elution results, tris and D-sorbitol produced similar protein elution from the column, suggesting that cis-diol affinity bonding, enhanced by coordination secondary interaction, is in fact the driving force for retention of the target molecules tested.

Given the results obtained for fragments derived from polyclonal antibody mixture, aminophenylboronate could still be used in the downstream processing of kappa and lambda Fabs, but only in two situations: the fragments are expressed in CHO-S cells and will totally binds to the ligand while impurity proteins from the cell culture supernatant are wash-out or the fragment is produced by enzymatic cleavage and it remains in the FT fraction while Fc fragments and undigested antibody bind to the column. Either way, further studies would be required to confirm these possibilities, including an ELISA assay using antibodies for different isotypes, combined with a case-by-case analysis of commercially relevant molecules. Also, it would be important to confirm if the chromatographic conditions here used do not significantly change protein tertiary structure, by circular dichroism, and its bioactivity, by studying fragments affinity towards respective antigen. Lastly, to confirm the key importance of cis-diol affinity bonding for retention of antibody derived-fragments to aminophenylboronate, it would be interesting to compare adsorption of glycosylated and non-glycosylated proteins. For this, the use of commercially available kits for protein deglycosylation could be used to remove carbohydrate groups from antibody fragments.

References

1. Lipman, N. S., Jackson, L. R., Trudel, L. J., *et al.* Monoclonal Versus Polyclonal Antibodies: Distinguishing Characteristics, Applications, and Information Resources. *ILAR J.* **46**, 258–268 (2005).

2. Steeland, S., Vandenbroucke, R. E. & Libert, C. Nanobodies as therapeutics: Big opportunities for small antibodies. *Drug Discov. Today* **21**, 1076–1113 (2016).

3. Rodrigo, G., Gruvegård, M. & Van Alstine, J. Antibody Fragments and Their Purification by Protein L Affinity Chromatography. *Antibodies* **4**, 259–277 (2015).

4. Spitali, M. Downstream processing of monocloanl antibody fragments. in *Process Scale Purification of Antibodies* (U. Gottschalk (Ed.), 2017).

5. Brena, B. M., Batista-Viera, F., Rydén, L., *et al.* Selective adsorption of immunoglobulins and glucosylated proteins on phenylboronate-agarose. *J. Chromatogr. A* **604**, 109–115 (1992).

6. Azevedo, A. M., Gomes, A. G., Borlido, L., *et al.* Capture of human monoclonal antibodies from a clarified cell culture supernatant by phenyl boronate chromatography. *J. Mol. Recognit.* **23**, 569–576 (2010).

7. Nascimento, A., Pinto, I. F., Chu, V., *et al.* Studies on the purification of antibody fragments. *Sep. Purif. Technol.* **195**, 388–397 (2018).

8. Pinto, I. F., Soares, R. R. G., Rosa, S. A. S. L., *et al.* High-Throughput Nanoliter-Scale Analysis and Optimization of Multimodal Chromatography for the Capture of Monoclonal Antibodies. *Anal. Chem.* **88**, 7959–7967 (2016).

9. Janda, A., Bowen, A., Greenspan, N. S., *et al.* Ig constant region effects on variable region structure and function. *Front. Microbiol.* **7**, 1–10 (2016).

10. Arruebo, M., Valladares, M. & González-Fernández, Á. Antibody-conjugated nanoparticles for biomedical applications. *J. Nanomater.* **2009**, 1–24 (2009).

11. Janeway CA Jr, Travers P, Walport M, et al. *Immunobiology: The Immune System in Health and Disease*. (Garland Science, 2001).

12. Weisser, N. E. & Hall, J. C. Applications of single-chain variable fragment antibodies in therapeutics and diagnostics. *Biotechnol. Adv.* **27**, 502–520 (2009).

13. Sanz, L., Cuesta, Á. M., Compte, M., *et al.* Antibody engineering: Facing new challenges in cancer therapy. *Acta Pharmacol. Sin.* **26**, 641–648 (2005).

14. Bondt, A., Rombouts, Y., Selman, M. H. J., *et al.* Immunoglobulin G (IgG) Fab Glycosylation Analysis Using a New Mass Spectrometric High-throughput Profiling Method Reveals Pregnancy-associated Changes. *Mol. Cell. Proteomics* **13**, 3029–3039 (2014).

15. Irani, V., Guy, A. J., Andrew, D., *et al.* Molecular properties of human IgG subclasses and their implications for designing therapeutic monoclonal antibodies against infectious diseases. *Mol. Immunol.* **67**, 171–182 (2015).

16. van de Bovenkamp, F. S., Hafkenscheid, L., Rispens, T., *et al.* The Emerging Importance of IgG Fab Glycosylation in Immunity. *J. Immunol.* **196**, 1435–1441 (2016).

17. Kiyoshi, M., Tsumoto, K., Ishii-Watabe, A., *et al.* Glycosylation of IgG-Fc: A molecular perspective. *Int. Immunol.* **29**, 311–317 (2017).

18. Parekh R, Roitt I, Isenberg D, Dwek R, R. T. Age-Related Galastosylation of the N-Linked Oligosaccharides of Human Serum IgG. *J. Exp. Med. JEM* **167**, 1731–1736 (1988).

19. Van de Geijn, F. E., Wuhrer, M., Selman, M. H. J., *et al.* Immunoglobulin G galactosylation and sialylation are associated with pregnancy-induced improvement of rheumatoid arthritis and the postpartum flare: Results from a large prospective cohort study. *Arthritis Res. Ther.* **11**, 1–10 (2009).

20. RB Parekh, Dwek, R. & Sutton, B. Association of rheumatoid arthritis and primary osteoarthriris with changes in the glycosylation pattern of total serum IgG. *Nature* **316**, 452–457 (1985).

21. Russell, A., Adua, E., Ugrina, I., *et al.* Unravelling immunoglobulin G Fc N-glycosylation: A dynamic marker potentiating predictive, preventive and personalised medicine. *Int. J. Mol. Sci.* **19**, 390 (2018).

22. Mimura, Y., Ashton, P. R., Takahashi, N., *et al.* Contrasting glycosylation profiles between Fab and Fc of a human IgG protein studied by electrospray ionization mass spectrometry. *J. Immunol. Methods* **326**, 116–126 (2007).

23. Anumula, K. R. Quantitative glycan profiling of normal human plasma derived immunoglobulin and its fragments Fab and Fc. *J. Immunol. Methods* **382**, 167–176 (2012).

24. Nuñez-Prado, N., Compte, M., Harwood, S., *et al.* The coming of age of engineered multivalent antibodies. *Drug Discov. Today* **20**, 588–594 (2015).

25. Krah, S., Schröter, C., Zielonka, S., *et al.* Single-domain antibodies for biomedical applications. *Immunopharmacol. Immunotoxicol.* **38**, 21–28 (2016).

26. Richards, D. A., Maruani, A. & Chudasama, V. Antibody fragments as nanoparticle targeting ligands: a step in the right direction. *Chem. Sci.* **8**, 63–77 (2016).

27. Porter, B. Y. R. R. The hydrolysis of rabbit Y-globulin and antibodies with crystalline papain. *Biochem. J.* **73**, 119–127 (1956).

28. Saeed, A. F. U. H., Wang, R., Ling, S., *et al.* Antibody engineering for pursuing a healthier future. *Front. Microbiol.* **8**, 1–28 (2017).

29. Nelson, A. L. Antibody fragments: Hope and hype. *MAbs* **2**, 77–83 (2010).

30. Kontermann, R. E. Strategies for extended serum half-life of protein therapeutics. *Curr. Opin. Biotechnol.* **22**, 868–876 (2011).

31. Holt, L. J., Basran, A., Jones, K., *et al.* Anti-serum albumin domain antibodies for extending the half-lives of short lived drugs. *Protein Eng. Des. Sel.* **21**, 283–288 (2008).

32. Nguyen, A., Reyes, A. E., Zhang, M., *et al.* The pharmacokinetics of an albumin-binding Fab (AB.Fab) can be modulated as a function of affinity for albumin. *Protein Eng. Des. Sel.* **19**, 291–297 (2006).

33. Berg, K., Pedersen, T. R., Sandvik, L., *et al.* Comparison of ranibizumab and bevacizumab for neovascular age-related macular degeneration according to LUCAS treat-and-extend protocol. *Ophthalmology* **122**, 146–152 (2015).

34. Moja, L., Lucenteforte, E., Kwag, KH., *et al.* Systemic safety of bevacizumab versus ranibizumab for neovascular age-related macular degeneration. *Cochrane Database Syst Rev* **85**, 1–27 (2015).

35. Moreno, T. A. & Kim, S. J. Ranibizumab (Lucentis) versus Bevacizumab (Avastin) for the Treatment of Age-Related Macular Degeneration: An Economic Disparity of Eye Health. *Semin. Ophthalmol.* **31**, 378–384 (2016).

36. Kovach, J. L., Schwartz, S. G., Flynn, H. W., *et al.* Anti-VEGF treatment strategies for wet AMD. *J. Ophthalmol.* **2012**, (2012).

37. Schauwvlieghe, A. M. E., Dijkman, G., Hooymans, J. M., *et al.* Comparing the effectiveness of bevacizumab to ranibizumab in patients with exudative age-related macular degeneration. The BRAMD study. *PLoS One* **11**, 1–16 (2016).

38. Kodjikian, L., Decullier, E., Souied, E. H., *et al.* Bevacizumab and ranibizumab for neovascular age-related macular degeneration: an updated meta-analysis of randomised clinical trials. *Graefe's Arch. Clin. Exp. Ophthalmol.* **252**, 1529–1537 (2014).

39. Zhao, Y., Gutshall, L., Jiang, H., *et al.* Two routes for production and purification of Fab fragments in biopharmaceutical discovery research: Papain digestion of mAb and transient expression in mammalian cells. *Protein Expr. Purif.* **67**, 182–189 (2009).

40. Andrew, SM., Titus, J. Fragmentation of Immunoglobulin G. in *Current Protocols in Cell Biology* vol. 17 16.4.1-16.4.10 (2003).

41. Wang, A. C. & Wang, I. Y. Cleavage sites of human IgGl immunoglobulin by papain. *Immunochemistry* **14**, 197–200 (1977).

42. Camper, N., Byrne, T., Burden, R. E., *et al.* Stable expression and purification of a functional processed Fab' fragment from a single nascent polypeptide in CHO cells expressing the mCAT-1 retroviral receptor. *J. Immunol. Methods* **372**, 30–41 (2011).

43. Jalalirad, R. Production of antibody fragment (Fab) throughout Escherichia coli fed-batch fermentation process: Changes in titre, location and form of product. *Electron. J. Biotechnol.* **16**, (2013).

44. Burtet, R. T., Santos-Silva, M. A., Buss, G. A. M., *et al.* Production of a recombinant Fab in Pichia pastoris from a monocistronic expression vector. *J. Biochem.* **142**, 665–669 (2007).

45. Backovic, M., Johansson, D. X., Klupp, B. G., *et al.* Efficient method for production of high yields of Fab fragments in Drosophila S2 cells. *Protein Eng. Des. Sel.* **23**, 169–174 (2010).

46. De Wilde, C., Peeters, K., Jacobs, A., *et al.* Expression of antibodies and Fab fragments in transgenic potato plants: A case study for bulk production in crop plants. *Mol. Breed.* **9**, 271–282 (2002).

47. Frenzel, A., Hust, M. & Schirrmann, T. Expression of recombinant antibodies. *Front. Immunol.* **4**, 1–20 (2013).

48. Schatz, S. M., Kerschbaumer, R. J., Gerstenbauer, G., *et al.* Higher Expression of Fab Antibody Fragments in a CHU Cell Line at Reduced Temperature. *Biotechnol. Bioeng.* **84**, 433–438 (2003).

49. Liu, H. F., Ma, J., Winter, C., *et al.* Recovery and purification process development for monoclonal antibody production. *MAbs* **2**, 480–499 (2010).

50. Kruljec, N. & Bratkovič, T. Alternative Affinity Ligands for Immunoglobulins. *Bioconjug. Chem.* **28**, 2009–2030 (2017).

51. Eifler, N., Medaglia, G., Anderka, O., *et al.* Development of a novel affinity chromatography resin for platform purification of lambda fabs. *Biotechnol. Prog.* **30**, 1311–1318 (2014).

52. Ma, H. & O'Kennedy, R. Recombinant antibody fragment production. *Methods* **116**, 23–33 (2017).

53. Mhatre, R., Nashabeh, W., Schmalzing, D., *et al.* Purification of antibody Fab fragments by cation-exchange chromatography and pH gradient elution. *J. Chromatogr. A* **707**, 225–231 (1995).

54. Kallberg, K., Johansson, H. O. & Bulow, L. Multimodal chromatography: An efficient tool in downstream processing of proteins. *Biotechnol. J.* **7**, 1485–1495 (2012).

55. Hjerten, S., Levin, O. & Tiselius, A. Protein chromatography on calcium phosphate columns. *Arch. Biochem. Biophys.* **65**, 132 (1956).

56. Pinto, I. F., Aires-Barros, M. R. & Azevedo, A. M. Multimodal chromatography: debottlenecking the downstream processing of monoclonal antibodies. *Pharm. Bioprocess.* **3**, 263–279 (2015).

57. Zhao, G., Dong, X. Y. & Sun, Y. Ligands for mixed-mode protein chromatography: Principles, characteristics and design. *J. Biotechnol.* **144**, 3–11 (2009).

58. Li, D., Chen, Y. & Liu, Z. Boronate affinity materials for separation and molecular recognition: Structure, properties and applications. *Chem. Soc. Rev.* **44**, 8097–8123 (2015).

59. Middle, F. A., Bannister, A., Bellingham, A. J., *et al.* Separation of glycosylated haemoglobins using immobilized phenylboronic acid. Effect of ligand concentration, column operating conditions, and comparison with ion-exchange and isoelectric-focusing. *Biochem. J.* **209**, 771–779 (1983).

60. Ivanov, A. E., Panahi, H. A., Kuzimenkova, M. V., *et al.* Affinity adhesion of carbohydrate particles and yeast cells to boronatecontaining polymer brushes grafted onto siliceous supports. *Chem. - A Eur. J.* **12**, 7204–7214 (2006).

61. Gomes, A. G., Azevedo, A. M., Aires-Barros, M. R., *et al.* Studies on the adsorption of cell impurities from plasmid-containing lysates to phenyl boronic acid chromatographic beads. *J. Chromatogr. A* **1218**, 8629–8637 (2011).

62. Carvalho, R. J., Woo, J., Aires-Barros, M. R., *et al.* Phenylboronate chromatography selectively separates glycoproteins through the manipulation of electrostatic, charge transfer, and cis-diol interactions. *Biotechnol. J.* **9**, 1250–1258 (2014).

63. Dhadge, V. L., Hussain, A., Azevedo, A. M., *et al.* Boronic acid-modified magnetic materials for antibody purification. *J. R. Soc. Interface* **11**, (2014).

64. dos Santos, R., Rosa, S. A. S. L., Aires-Barros, M. R., *et al.* Phenylboronic acid as a multi-modal ligand for the capture of monoclonal antibodies: Development and optimization of a washing step. *J. Chromatogr. A* **1355**, 115–124 (2014).

65. Springsteen, G. & Wang, B. A detailed examination of boronic acid ± diol complexation. *Tetrahedron* **58**, 5291–5300 (2002).

66. LIU, X. C. Boronic Acids as Ligands for Affinity Chromatography. *Chinese J. Chromatogr.* **24**, 73–80 (2006).

67. Li, X., Pennington, J., Stobaugh, J. F., *et al.* Synthesis of sulfonamide- and sulfonyl-phenylboronic acid-modified silica phases for boronate affinity chromatography at physiological pH. *Anal. Biochem.* **372**, 227–236 (2008).

68. Ren, L., Liu, Z., Dong, M., *et al.* Synthesis and characterization of a new boronate affinity monolithic capillary for specific capture of cis-diol-containing compounds. *J. Chromatogr. A* **1216**, 4768–4774 (2009).

69. Li, D., Li, Q., Wang, S., *et al.* Pyridinylboronic acid-functionalized organic-silica hybrid monolithic capillary for the selective enrichment and separation of cis-diol-containing biomolecules at acidic pH. *J. Chromatogr. A* **1339**, 103–109 (2014).

70. Zhang, B., Mathewson, S. & Chen, H. Two-dimensional liquid chromatographic methods to examine phenylboronate interactions with recombinant antibodies. *J. Chromatogr. A* **1216**,

5676–5686 (2009).

71. Mateus, M., Aires-barros, M. R. & Azevedo, A. M. Monoclonal antibodies production platforms : an opportunity study of a non-protein-A chromatographic platform based on process economics. *Biotechnol. J.* **12**, 1–23 (2017).

72. Rosa, S. A. S. L., da Silva, C. L., Aires-Barros, M. R., *et al.* Thermodynamics of the adsorption of monoclonal antibodies in phenylboronate chromatography: Affinity versus multimodal interactions. *J. Chromatogr. A* **1569**, 118–127 (2018).

73. Rosa, S. A. S. L., Wagner, A., da Silva, C. L., *et al.* Mobile phase modulators as salt tolerance enhancers in phenylboronate chromatography: thermodynamic evaluation of the mechanisms underlying the adsorption of monoclonal antibodies. *Biotechnol. J.* 0–2 (2019) doi:10.1002/biot.201800586.

74. Chhatre, S. & Titchener-Hooker, N. J. Review: Microscale methods for high-throughput chromatography development in the pharmaceutical industry. *J. Chem. Technol. Biotechnol.* **84**, 927–940 (2009).

75. Treier, K., Hansen, S., Richter, C., *et al.* High-throughput methods for miniaturization and automation of monoclonal antibody purification processes. *Biotechnol. Prog.* **28**, 723–732 (2012).

76. Petroff, M. G., Bao, H., Welsh, J. P., *et al.* High throughput chromatography strategies for potential use in the formal process characterization of a monoclonal antibody. *Biotechnol. Bioeng.* **113**, 1273–1283 (2016).

77. Coffman, J. L., Kramarczyk, J. F. & Kelley, B. D. High-throughput screening of chromatographic separations: I. method development and column modeling. *Biotechnol. Bioeng.* **100**, 605–618 (2008).

78. Welsh, J. P., Petroff, M. G., Rowicki, P., *et al.* A practical strategy for using miniature chromatography columns in a standardized high-throughput workflow for purification development of monoclonal antibodies. *Biotechnol. Prog.* **30**, 626–635 (2014).

79. Huft, J., Haynes, C. A. & Hansen, C. L. Microfluidic Integration of Parallel Solid-Phase Liquid Chromatography. *Anal. Chem.* **85**, 2999–3005 (2013).

80. Pinto, I. F., Caneira, C. R. F., Soares, R. R. G., *et al.* The application of microbeads to microfluidic systems for enhanced detection and purification of biomolecules. *Methods* **116**, 112–124 (2017).

81. BDP TMR NHS ester. https://www.lumiprobe.com/p/bodipy-tmr-nhs-ester.

82. Pinto, I. F., Rosa, S. A. S. L., Aires-barros, M. R., *et al.* Exploring the use of heparin as a first capture step in the purification of monoclonal antibodies from cell culture supernatants. *Biochem. Eng. J.* **104**, 27–33 (2015).

83. Kinman, A., W. L., & Pompano, R. R. Optimization of Enzymatic Antibody Fragmentation for Yield, Efficiency, and Binding Affinity. *Bioconjug. Chem.* acs.bioconjchem.8b00912 (2019) doi:10.1021/acs.bioconjchem.8b00912.

84. Dennison, TJ., Smith, J., Hofmann, MP., *et al*. Design of Experiments to Study the Impact of Process Parameters on Droplet Size and Development of Non-Invasive Imaging Techniques in Tablet Coating. *PLoS One* **11**, e0157267 (2016).

85. São Pedro, M. N., Azevedo, A. M., Aires-barros, M. R., *et al.* Minimizing the influence of fluorescent tags on IgG partition in PEG-salt aqueous two-phase systems for rapid screening applications. *Biotechnol. J.* **14**, (2019).

86. Hirano, A., Shiraki, K. & Tomoshi, K. Effects of Arginine on Multimodal Chromatography: Experiments and Simutions. *Current protein and peptide science*. **20**, 40-48 (2019).

87. Shukla, D., Zamolo, L., Cavallotti, C., *et al.* Understanding the Role of Arginine as an Eluent in Affinity Chromatography via Molecular Computations. *J. Phys. Chem.* **115**, 2645–2654 (2011).

Appendix

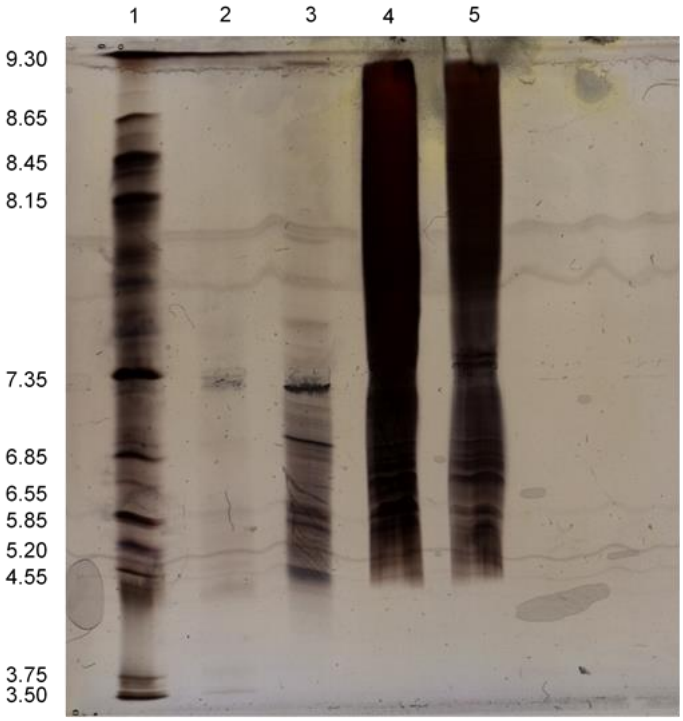

Figure A1. Isoelectric focusing gel of CHO-S supernatant proteins and Gammanorm® polyclonal mixture **1 -** Marker; **2** - Labelled CHO-S supernatant proteins **3** - Non-labelled CHO-S supernatant proteins; **4** - Labelled Gammanorm® **5** - Non-labelled Gammanorm®.

Table A1. Slope values for the first 15 seconds of elution of kappa and lambda Fabs from aminophenylboronate, using a concentration ranging from 0 to 2 M of Tris-HCl pH 8.5. Adsorption was performed using 50 mM Phosphate buffer, which was also used as a negative control in the elution step.

	Kappa Fabs	**Lambda Fabs**
0.050 M Phosphate Buffer pH 7.0	-0.31 %/s	-0.47 %/s
0.250 M Tris pH 8.5	-2.64 %/s	-1.51 %/s
0.500 M Tris pH 8.5	-3.36 %/s	-2.42 %/s
0.750 M Trisl pH 8.5	-2.56 %/s	-3.41 %/s
1.00 M Tris pH 8.5	-2.87 %/s	-3.95 %/s
1.25 M Tris pH 8.5	-2.64 %/s	-3.94 %/s
1.50 M Tris pH 8.5	-3.30 %/s	-3.93 %/s
1.75 M Tris pH 8.5	-2.88 %/s	-4.32 %/s
2.00 M Tris pH 8.5	-2.88 %/s	-3.66 %/s

Table A2. Slope values for the first 15 seconds of elution of kappa and lambda Fabs from aminophenylboronate, using a concentration ranging from 0 to 2 M of D-Sorbitol pH 8.5. 150 mM Tris-HCl was used to maintain the pH. Adsorption was performed using 50 mM Phosphate buffer, which was also used as a negative control in the elution step.

	Kappa Fabs	Lambda Fabs
0.050 M Phosphate Buffer pH 7.0	-0.31 %/s	-0.45 %/s
0.150 M Tris-HCl 0.250 M Sorbitol pH 8.5	-1.76 %/s	-1.40 %/s
0.150 M Tris-HCl 0.500 M Sorbitol pH 8.5	-1.88 %/s	-1.26 %/s
0.150 M Tris-HCl 0.750 M Sorbitol pH 8.5	-1.38 %/s	-1.25 %/s
0.150 M Tris-HCl 1.00 M Sorbitol pH 8.5	-2.01 %/s	-1.22 %/s
0.150 M Tris-HCl 1.25 M Sorbitol pH 8.5	-1.38 %/s	-1.50 %/s
0.150 M Tris-HCl 1.50 M Sorbitol pH 8.5	-1.11 %/s	-3.00 %/s
0.150 M Tris-HCl 1.75 M Sorbitol pH 8.5	-0.85 %/s	-2.45 %/s
0.150 M Tris-HCl 2.00 M Sorbitol pH 8.5	-0.85 %/s	-1.39 %/s

Table A3. Slope values for the first 15 seconds of elution of kappa and lambda Fabs from aminophenylboronate, using a concentration ranging from 0 to 1 M of Arginine pH 8.5. 150 mM Tris-HCl was used to maintain the pH. Adsorption was performed using 50 mM Phosphate buffer, which was also used as a negative control in the elution step.

	Kappa Fabs	Lambda Fabs
0.05 M Phosphate Buffer pH 7.0	-0.63 %/s	-0.66 %/s
0.15 M Tris-HCl 0.25 M Arginine pH 8.5	-1.66 %/s	-2.63 %/s
0.15 M Tris-HCl 0.50 M Arginine pH 8.5	-2.87 %/s	-4.01 %/s
0.15 M Tris-HCl 0.75 M Arginine pH 8.5	-2.50 %/s	-3.97 %/s
0.15 M Tris-HCl 1.00 M Arginine pH 8.5	-2.38 %/s	-3.52 %/s

Table A4. Slope values for the first 15 seconds of elution of kappa and lambda Fabs from aminophenylboronate, using a concentration ranging from 0 to 2 M of Magnesium Chloride pH 8.5. 150 mM Tris-HCl was used to maintain the pH. Adsorption was performed using 50 mM Phosphate buffer, which was also used as a negative control in the elution step.

	Kappa Fabs	Lambda Fabs
0.050 M Phosphate Buffer pH 7.0	-0.58 %/s	-0.43 %/s
0.150 M Tris-HCl 0.250 M $MgCl_2$ pH 8.5	-2.62 %/s	-1.31 %/s
0.150 M Tris-HCl 0.500 M $MgCl_2$ pH 8.5	-2.60 %/s	-0.80 %/s
0.150 M Tris-HCl 0.750 M $MgCl_2$ pH 8.5	-2.41 %/s	-1.19 %/s
0.150 M Tris-HCl 1.00 M $MgCl_2$ pH 8.5	-2.37 %/s	-0.99 %/s
0.150 M Tris-HCl 1.25 M $MgCl_2$ pH 8.5	-1.69 %/s	-0.56 %/s
0.150 M Tris-HCl 1.50 M $MgCl_2$ pH 8.5	-2.11 %/s	-0.89 %/s
0.150 M Tris-HCl 1.75 M $MgCl_2$ pH 8.5	-1.49 %/s	-0.50 %/s
0.150 M Tris-HCl 2.00 M $MgCl_2$ pH 8.5	-1.58 %/s	-0.43 %/s

Table A5. Slope values for the first 15 seconds of elution of kappa and lambda Fabs from aminophenylboronate, using a concentration ranging from 0 to 1 M of Guanidine Hydrochloride pH 8.5. 150 mM Tris-HCl was used to maintain the pH. Adsorption was performed using 50 mM Phosphate buffer, which was also used as a negative control in the elution step.

	Kappa Fabs	**Lambda Fabs**
0.050 M Phosphate Buffer pH 7.0	-0.26 %/s	-0.44 %/s
0.15 M Tris-HCl 0.25 M Guanidine hydrochloride pH 8.5	-1.29 %/s	-3.14 %/s
0.15 M Tris-HCl 0.50 M Guanidine hydrochloride pH 8.5	-2.04 %/s	-3.49 %/s
0.15 M Tris-HCl 0.75 M Guanidine hydrochloride pH 8.5	-2.69 %/s	-3.40 %/s
0.15 M Tris-HCl 1.00 M Guanidine hydrochloride pH 8.5	-2.96 %/s	-3.70 %/s

Table A6. Slope values for the first 15 seconds of elution of kappa and lambda Fabs from aminophenylboronate, using a concentration ranging from 0 to 1 M of Urea pH 8.5. 150 mM Tris-HCl was used to maintain the pH. Adsorption was performed using 50 mM Phosphate buffer, which was also used as a negative control in the elution step.

	Kappa Fabs	**Lambda Fabs**
0.050 M Phosphate Buffer pH 7.0	-0.25 %/s	-0.41 %/s
0.15 M Tris-HCl 0.25 M Urea pH 8.5	-1.21 %/s	-2.33 %/s
0.15 M Tris-HCl 0.50 M Urea pH 8.5	-0.81 %/s	-2.75 %/s
0.15 M Tris-HCl 0.75 M Urea pH 8.5	-1.67 %/s	-2.72 %/s
0.15 M Tris-HCl 1.00 M Urea pH 8.5	-1.54 %/s	-2.50 %/s